J|A|C|S
ARTICLES
Published on Web 04/08/2003

Polyunsaturated Dicarboxylate Tethers Connecting Dimolybdenum Redox and Chromophoric Centers: Syntheses, Structures, and Electrochemistry

F. Albert Cotton,* James P. Donahue,* and Carlos A. Murillo*

Contribution from the Department of Chemistry, Laboratory for Molecular Structure and Bonding, P.O. Box 30012, Texas A&M University, College Station, Texas 77842-3012

Received October 25, 2002; E-mail: cotton@tamu.edu; donahue@lmsb.tamu.edu; murillo@tamu.edu

Abstract: Compounds with two quadruply bonded Mo_2^{4+} units, $Mo_2(DAniF)_3$ (DAniF = *N,N′*-di-*p*-anisylformamidinate), linked by unsaturated dicarboxylate dianions of various lengths have been prepared and their spectroscopic and electrochemical properties studied. As identified by the dicarboxylate linkers, these compounds are maleate (**7**), allene-1,3-dicarboxylate (**10**), *cis,cis*-muconate (**11**), *trans,trans*-muconate (**12**), octa-2,4,6-*trans,trans,trans*-hexatriene-1,8-dioate (tamuate, **13**), and deca-2,4,6,8-*trans,trans,trans,-trans*-octatetraene-1,10-dioate (texate, **14**). The latter three molecules complete the five-membered (all *trans*) series $[Mo_2(DAniF)_3](O_2C(CH{=}CH)_nCO_2)[Mo_2(DAniF)_3]$ ($n = 0-4$). Several unsymmetrical paddle-wheel compounds of the type $Mo_2(DAniF)_3(O_2CX)$ (X = C≡CH (**3**), CH=CH_2 (**4**), (*E*)-CH=CH−CH=CH_2 (**5**)) have also been prepared for comparison to the molecules in which there are linked Mo_2 units. The precursors $[Mo_2(DAniF)_3(MeCN)_2](BPh_4)$, [**1**]$BPh_4$, and $Mo_2(DAniF)_3Cl(MeCN)$ (**2**) have also been isolated and characterized. The structures of all new molecules have been established by X-ray crystallography, including the methyl esters of various carboxylates used as ligands. All of the linked molecules have been examined by cyclic and differential pulse voltammetry, and $\Delta E_{1/2}$ values, the separation between successive Mo_2^{4+}/Mo_2^{5+} oxidations, have been determined. Those compounds with highly unsaturated, fully conjugated linkers demonstrate electrochemical communication from end-to-end that is more persistent over distance than is accounted for by an electrostatic interaction alone, implying that the π system of these dicarboxylate linkers is mediating communication. In the series $[Mo_2(DAniF)_3](O_2C(CH{=}CH)_nCO_2)[Mo_2(DAniF)_3]$ ($n = 0-4$), the first oxidation potential shifts progressively to less positive values due to an increasing contribution of the polyolefinic α,ω-dicarboxylate to the molecular orbital undergoing oxidation. This first oxidation potential approaches a limiting value of 63 mV (vs Ag/AgCl) as *n* becomes infinitely long. Compound **11** can be photoisomerized to **12** in a process that is affected by the presence of the Mo_2^{4+} units, as the analogous rearrangement of dimethyl *cis,cis*-muconate is faster.

Introduction

Electronic communication between two atoms or two groups of atoms is a process fundamental to numerous complex chemical systems ranging from life processes[1] to photoactive donor/acceptor processes[2] and electronic devices.[3] In a system with multiple components, it is crucial to understand how the transfer of electrons from one subunit to another is affected by many possible variables so that this can allow fine-tuning of the intrinsic chemical characteristics that will lead to improved electronic and excitonic performance. However, studies of this nature are often complicated by characteristics of the linker, including conformational ones.[4]

There are many ways of probing electronic communication between components connected by linkers, such as studying their magnetic properties,[5] their response to electromagnetic radiation,[6] or their electrochemical behavior.[7] The pioneering studies by Taube on the Creutz−Taube type complexes having two linked ruthenium ions are a paradigm for work in this field.[8] Such research still constitutes an important area of chemical

(1) For example, see: (a) Lippard, S. J.; Berg, J. M. *Principles of Bioinorganic Chemistry*; University Science Books: Mill Valley, California, 1994. (b) Schuster, G. B. *Acc. Chem. Res.* **2000**, *33*, 253.
(2) (a) Endicott, J. F.; Kumar, K.; Ramasami, T.; Rotzinger, F. P. *Prog. Inorg. Chem.* **1983**, *30*, 141. (b) Barigelletti, F.; Flamigni, L. *Chem. Soc. Rev.* **2000**, *29*, 1.
(3) (a) Wosnick, J. H.; Swager, T. M. *Curr. Opin. Chem. Biol.* **2000**, *4*, 715. (b) Tour, J. M.; Rawlett, A. M.; Kozaki, M.; Yao, Y.; Jagessar, R. C.; Dirk, S. M.; Price, D. W.; Reed, M. A.; Zhou, C.-W.; Chen, J.; Wang, W.; Campbell, I. *Chem.−Eur. J.* **2001**, *7*, 5118. (c) Launay, J.-P. *Chem. Soc. Rev.* **2001**, *30*, 386. (d) Cahen, D.; Hodes, G. *Adv. Mater.* **2002**, *14*, 789. (e) Ratner, M. A. *Mater. Today* **2002**, *5*, 20. (f) Kwok, K. S.; Ellenbogen, J. C. *Mater. Today* **2002**, *5*, 28.
(4) (a) Ortega, J. V.; Hong, B.; Ghosal, S.; Hemminger, J. C.; Breedlove, B.; Kubiak, C. P. *Inorg. Chem.* **1999**, *38*, 5102. (b) Chisholm, M. H. *Acc. Chem. Res.* **2000**, *33*, 53.
(5) (a) Kahn, O. *Molecular Magnetism*; Wiley−VCH: New York, 1993. (b) Seddon, E. J.; Yoo, J.; Folting, K.; Huffman, J. C.; Hendrickson, D. N.; Christou, G. *J. Chem. Soc., Dalton Trans.* **2000**, 3640. (c) Sañudo, E. C.; Grillo, V. A.; Knapp, M. J.; Bollinger, J. C.; Huffman, J. C.; Hendrickson, D. N.; Christou, G. *Inorg. Chem.* **2002**, *41*, 2441.
(6) (a) Pourtois, G.; Beljonne, D.; Cornil, J.; Ratner, M. A.; Brédas, J. L. *J. Am. Chem. Soc.* **2002**, *124*, 4436. (b) Niyogi, K. K. *Curr. Opin. Plant Biol.* **2000**, *3*, 455.
(7) For example, see: Richardson, D. E.; Taube, H. *Inorg. Chem.* **1981**, *20*, 1278.
(8) (a) Creutz, C. *Prog. Inorg. Chem.* **1983**, *30*, 1. (b) Brunschwig, B. S.; Creutz, C.; Sutin, N. *Chem. Soc. Rev.* **2002**, *31*, 168.

 10.1021/ja029101i CCC: $25.00 **© 2003 American Chemical Society**

investigation today. Electron-transfer processes between two redox centers have been examined with various linkers such as simple monatomic units,[9] inorganic anions such as MO_4^{2-} groups (M = S, Mo, W)[10] or CO_3^{2-} anions,[11] organic linkers such as polyynes,[12] polyenes including carotenoids,[13] polymeric π-conjugated organic frameworks,[14] polyphosphine/cumulene spacers,[4a] polyphenyls and polyaromatics,[15] ferrocenes,[16] multiporphyrins,[17] and dipyridylpolyenes.[18]

The major goals of research in this laboratory at present are four: (1) to increase the diversity of the metal centers that may be used, (2) to increase the diversity of linkers that may be used, (3) to design molecules that may have nanoscale applications, and (4) to elucidate the principles by which the behavior of all such systems is governed. In doing so, we have continued two of our own approaches, which are (a) to use dimetal units rather than single metal atoms[19] and (b) to connect them with dicarboxylic acids[19] and related species, for example, diamidates[20] and diamidinates.[21] We also continue to search for relationships between the nature of the organic matter that lies between the carboxylate groups and the extent to which excitation at one dimetal unit is coupled to analogous excitation at the other.

Dimetal units, which can be supported by two or three formamidinates, carboxylates, or other bridging ligands, offer many advantages over the mononuclear units. One advantage is that substitutions on the supporting ligands can have a large impact on the electronic properties of the dinuclear unit, notably on the electrochemistry. The latter is of special interest for compounds with Mo_2^{4+} units. These have a $\sigma^2\pi^4\delta^2$ electronic configuration and exhibit $\delta \rightarrow \delta^*$ transitions in the visible spectra which are highly dependent on the supporting ligands.[22] Additional advantages of using such Mo_2 units as internal probes arise not only from the well understood chemistry and spectroscopy but also because they offer multiple stable oxidations.[22]

Scheme 1. Generic Structure of a Dicarboxylate Linked Pair $Mo_2(DAniF)_3(O_2CXCO_2)[Mo_2(DAniF)_3]$, Including the Structure of the *N,N′*-di-*p*-anisylformamidinate (DAniF) Ligand

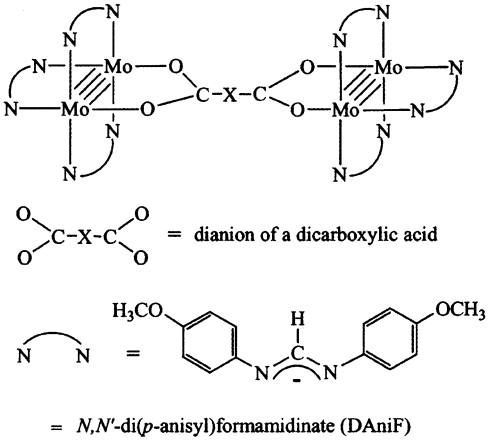

One indispensable key to success in the field is to devise and employ dimetal units that are not subject to rearrangements, disproportionations, or other interfering reactions. This is accomplished by choosing suitable supporting ligands. In recent studies, we have shown that quadruply bonded units of the type shown in Scheme 1 remain firmly intact when linked by dicarboxylate units of various types and that the oxidation potentials of such species are highly dependent upon the nature of the linker, especially its length and the presence or absence of unsaturation and bond conjugation.[23] We have shown that dimetal units may also be used to form supramolecular structures such as loops, triangles, squares, polygons, and other extended architectures, many of which exhibit significant electronic communication between the dimetal units as mediated by the linkers.[19]

In the first of two reports,[24] we present the synthesis and structural characterization of a series of compounds having two quadruply bonded $Mo_2(DAniF)_3$ (DAniF = *N,N′*-di-*p*-anisylformamidinate) units linked by dicarboxylate anions having chains of up to four alternating single and double bonds. We also show the structures of the precursors, both the metal containing units and the organic acids, as well as those of a group of unsymmetrical Mo_2^{4+} compounds having three formamidinate ligands and one carboxylate anion with unsaturated C−C bonds. For the pairs, we have studied how the conjugated dicarboxylates modulate the electronic communication between the two distal dimetal units separated by linkers having 0, 1, 2, 3, and 4 all *trans* carbon−carbon double bonds, and we have analyzed the effect of the dimetal units on the *cis*−*trans* isomerization of two C=C bonds on the linker.

(9) Villata, L. S.; Féliz, M. R.; Capparelli, A. L. *Coord. Chem. Rev.* **2000**, *196*, 65.
(10) Cotton, F. A.; Donahue, J. P.; Murillo, C. A. *Inorg. Chem.* **2001**, *40*, 2229.
(11) Cotton, F. A.; Lin, C.; Murillo, C. A. *J. Am. Chem. Soc.* **2001**, *123*, 2670.
(12) (a) Coat, F.; Lapinte, C. *Organometallics* **1996**, *15*, 477. (b) Dembinski, R.; Bartik, T.; Bartik, B.; Jaeger, M.; Gladysz, J. A. *J. Am. Chem. Soc.* **2000**, *122*, 810. (c) Ren, T.; Zou, G.; Alvarez, J. C. *Chem. Commun.* **2000**, 1197. (d) Wong, K.-T.; Lehn, J.-M.; Peng, S.-M.; Lee, G.-H. *Chem. Commun.* **2000**, 2259.
(13) (a) Arrhenius, T. S.; Blanchard-Desce, M.; Dvolaitzky, M.; Lehn, J.-M.; Malthete, J. *Proc. Natl. Acad. Sci. U.S.A.* **1986**, *83*, 5355. (b) Slama-Schwok, A.; Blanchard-Desce, M.; Lehn, J.-M. *J. Phys. Chem.* **1990**, *94*, 3894. (c) Etzenhouser, B. A.; Cavanaugh, M. D.; Spurgeon, H. N.; Sponsler, M. B. *J. Am. Chem. Soc.* **1994**, *116*, 2221. (d) Ribou, A.-C.; Launay, J.-P.; Sachtleben, M. L.; Li, H.; Spangler, C. W. *Inorg. Chem.* **1996**, *35*, 3735. (e) Hapiot, P.; Kispert, L. D.; Konovalov, V. V.; Savéant, J.-M. *J. Am. Chem. Soc.* **2001**, *123*, 6669.
(14) Kingsborough, R. P.; Swager, T. M. *Prog. Inorg. Chem.* **1999**, *48*, 123.
(15) (a) Lacoste, M.; Varret, F.; Toupet, L.; Astruc, D. *J. Am. Chem. Soc.* **1987**, *109*, 6504. (b) Collin, J.-P.; Lainé, P.; Launay, J.-P.; Sauvage, J.-P.; Sour, A. *J. Chem. Soc., Chem. Commun.* **1993**, 434. (c) Rabaâ, H.; Lacoste, M.; Delville-Desbois, M.-H.; Ruiz, J.; Gloaguen, B.; Ardoin, N.; Astruc, D.; Le Beuze, A.; Saillard, J.-Y.; Linares, J.; Varret, F.; Dance, J.-M.; Marquestaut, E. *Organometallics* **1995**, *14*, 5078. (d) Galán-Mascarós, J. R.; Dunbar, K. R. *Chem. Commun.* **2001**, 217. (e) Campos-Fernández, C. S.; Clérac, R.; Koomen, J. M.; Russell, D. H.; Dunbar, K. R. *J. Am. Chem. Soc.* **2001**, *123*, 773.
(16) (a) Morán, M.; Casado, C. M.; Cuadrado, I.; Losada, J. *Organometallics* **1993**, *12*, 4327. (b) Constable, E. C.; Edwards, A. J.; Marcos, M. D.; Raithby, P. R.; Martínez-Máñez, R.; Tendero, M. J. L. *Inorg. Chim. Acta* **1994**, *224*, 11. (c) Astruc, D. *Acc. Chem. Res.* **1997**, *30*, 383. (d) Alvarez, J.; Ren, T.; Kaifer, A. E. *Organometallics* **2001**, *20*, 3543. (e) Alvarez, J.; Ni, Y.; Ren, T.; Kaifer, A. E. *J. Supramol. Chem.* **2001**, *1*, 7. (f) Zakaria, C. M.; Ferguson, G.; Lough, A. J.; Glidewell, C. *Acta Crystallogr.* **2002**, *B58*, 786.
(17) (a) Crossley, M. J.; Burn, P. L. *J. Chem. Soc., Chem. Commun.* **1991**, 1569. (b) Iengo, E.; Zangrando, E.; Minatel, R.; Alessio, E. *J. Am. Chem. Soc.* **2002**, *124*, 1003.
(18) (a) Sutton, J. E.; Taube, H. *Inorg. Chem.* **1981**, *20*, 3125. (b) Woitellier, S.; Launay, J. P.; Spangler, C. W. *Inorg. Chem.* **1989**, *28*, 758. (c) Reimers, J. R.; Hush, N. S. *Inorg. Chem.* **1990**, *29*, 3686. (d) McWhinnie, S. L. W.; Thomas, J. A.; Hamor, T. A.; Jones, C. J.; McCleverty, J. A.; Collison, D.; Mabbs, F. E.; Harding, C. J.; Yellowlees, L. J.; Hutchings, M. G. *Inorg. Chem.* **1996**, *35*, 760.
(19) (a) Cotton, F. A.; Lin, C.; Murillo, C. A. *Acc. Chem. Res.* **2001**, *34*, 759. (b) Cotton, F. A.; Lin, C.; Murillo, C. A. *Proc. Natl. Acad. Sci. U.S.A.* **2002**, *99*, 4810.
(20) Cotton, F. A.; Daniels, L. M.; Donahue, J. P.; Liu, C. Y.; Murillo, C. A. *Inorg. Chem.* **2002**, *41*, 1354.
(21) Cotton, F. A.; Liu, C. Y.; Murillo, C. A. Unpublished results.
(22) Cotton, F. A.; Walton, R. A. *Multiple Bonds between Metal Atoms*; Clarendon: Oxford, 1993.
(23) Cotton, F. A.; Donahue, J. P.; Lin, C.; Murillo, C. A. *Inorg. Chem.* **2001**, *40*, 1234.
(24) The second report is in a succeeding paper in this issue: Cotton, F. A.; Donahue, J. P.; Murillo, C. A.; Pérez, L. M. *J. Am. Chem. Soc.* **2003**, *125*, 5486.

Chart 1. List of $Mo_2(DAniF)_3(O_2CX)$ and $[Mo_2(DAniF)_3]_2(\mu\text{-}O_2CXCO_2)$ Compounds as Identified by Their Mono- or Dicarboxylate Ligands

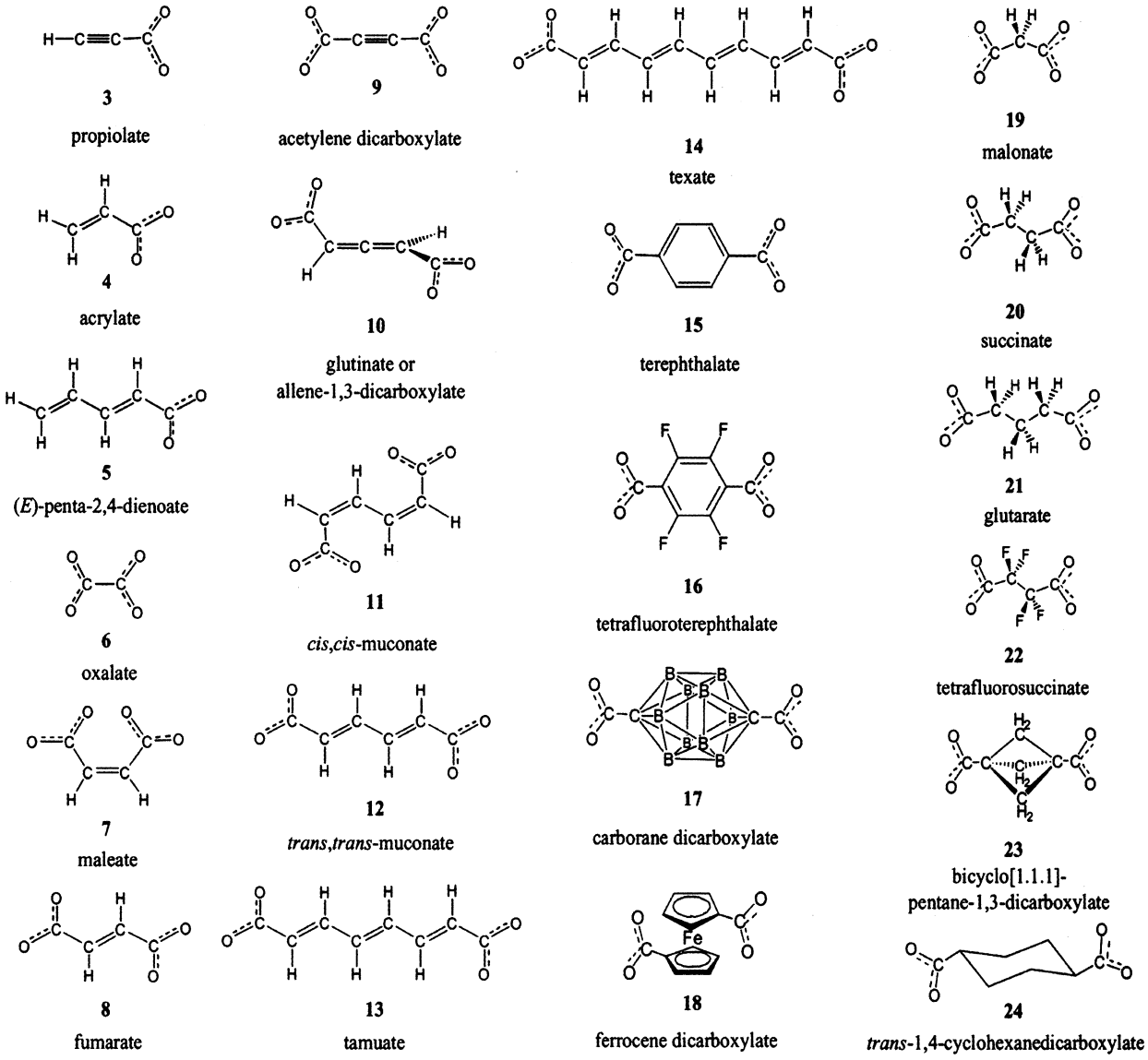

In the following report,[24] we discuss the manifestation of such communication using visible spectroscopy and show how DFT calculations help in understanding such experimental results.

Experimental Section

Materials and Methods. All manipulations and procedures were conducted under N_2 using either an N_2 drybox or standard Schlenk line techniques. Solvents were distilled and degassed immediately prior to use: MeCN was twice distilled under N_2, first from activated molecular sieves and then from CaH_2, MeOH was distilled from Mg(OMe)$_2$, CH_2Cl_2 and $ClCH_2CH_2Cl$ were dried and distilled from P_2O_5, and toluene, Et_2O, and hexanes were distilled from Na/K-benzophenone; 1,3-dichlorobenzene, 2,2,4-trimethylpentane, and Bu^{t}OMe were filtered through anhydrous Na_2SO_4 and degassed with vigorous N_2 bubbling. $Mo_2(DAniF)_3Cl_2$ was prepared according to the literature method,[25] and all tetraethylammonium dicarboxylate salts were prepared and isolated as white solids by neutralizing the corresponding diacid with 2 equiv of Et_4NOH followed by careful drying under vacuum.

The numbers in bold-faced type are used throughout the following discussion to designate $[Mo_2(DAniF)_3](O_2CXCO_2)[Mo_2(DAniF)_3]$ and $Mo_2(DAniF)_3(O_2CX)$ compounds, where the carboxylate ligands are those illustrated in Chart 1. The use of numbers followed by ***H**, ***H$_2$**, or ***Me$_2$** refers to the corresponding acids or to their methyl esters. Thus, for instance, the compound $[Mo_2(DAniF)_3](\mu\text{-}cis,cis\text{-}O_2C{-}(CH{=}CH)_2{-}CO_2)[Mo_2(DAniF)_3]$ is abbreviated as **11**, while *cis,cis*-$MeO_2C(CH{=}CH)_2CO_2Me$ (*cis,cis*-muconic acid dimethyl ester) is shortened to **11*Me$_2$**.

Allene-1,3-dicarboxylic acid (**10*H$_2$**) was prepared from 3-chloro-2-pentene dioic acid[26] according to the literature procedure.[27] Octa-*trans,trans,trans*-2,4,6-triene-1,8-dioic acid dimethyl ester[28] (tamuic acid dimethyl ester, **13*Me$_2$**) and (*E*)-penta-2,4-dienoic acid[29] (**5*H**) were similarly synthesized according to literature methods. Deca-*trans,trans,trans,trans*-2,4,6,8-tetraene-1,10-dioic acid (texic acid, **14*H$_2$**) was obtained by the base catalyzed rearrangement of deca-4,6-diyne-1,10-dioic acid,[30] which itself was prepared by the CuCl mediated coupling of 4-pentynoic acid.[31] The dimethyl ester of *cis,cis*-muconic acid was prepared by treatment of the corresponding dicarboxylate salt with

(25) Cotton, F. A.; Daniels, L. M.; Jordan, G. T., IV; Lin, C.; Murillo, C. A. *J. Am. Chem. Soc.* **1998**, *120*, 3398.
(26) Ikeda, I.; Honda, K.; Osawa, E.; Shiro, M.; Aso, M.; Kanematsu, K. *J. Org. Chem.* **1996**, *61*, 2031.
(27) van der Zanden, J. M. *Recl. Trav. Chim. Pays−Bas* **1935**, *54*, 289.
(28) Dreiding, A. S.; Pratt, R. J. *J. Am. Chem. Soc.* **1953**, *75*, 4580.
(29) Abarbri, M.; Parrain, J.-L.; Cintrat, J.-C.; Duchêne, A. *Synthesis* **1996**, 82.
(30) Jones, E. R. H.; Shaw, B. L.; Whiting, M. C. *J. Chem. Soc.* **1954**, 3212.
(31) Reppe, W. et al. *Justus Liebigs Ann. Chem.* **1955**, *596*, 72.

excess MeI in CH_2Cl_2/MeOH, while the *trans,trans* isomer was obtained by thermal isomerization of *cis,cis*-muconic acid dimethyl ester in hot MeOH. All other reagents were purchased from commercial sources and used as received. In this report, we are adopting short names for two acids with very cumbersome systematic names, namely $HO_2C(CH{=}CH)_nCO_2H$: tamuic acid ($n = 3$) and texic acid ($n = 4$).

Physical Methods. Elemental analyses were performed by Canadian Microanalytical Service, Delta, British Columbia, Canada, upon crystalline samples that were dried overnight under vacuum. In several instances, the presence of residual solvent was indicated by ^{1}H NMR and was factored into the expected analysis. ^{1}H NMR spectra were recorded on a Varian XL-200AA NMR spectrometer with chemical shifts referenced to the protonated solvent residual. Absorption spectra were measured at room temperature under N_2 using a Shimadzu UV-1601PC spectrophotometer. The cyclic voltammograms and differential pulse voltammograms were taken with a CH Instruments model-CH1620A electrochemical analyzer in 0.1 M Bu_4NPF_6 solution (CH_2Cl_2) with Pt working and auxiliary electrodes, a Ag/AgCl reference electrode, and a scan rate of 100 mV/s. All the potential values are referenced to the Ag/AgCl electrode, and under the present experimental conditions, the $E_{1/2}$ (Fc^+/Fc) consistently occurred at 440 mV.

X-ray Structures. Block-shaped crystals of 3-chloro-*cis*-2-pentene dioic acid and of **5*H** were obtained by slow evaporation of Et_2O solutions, while slow cooling of an Et_2O solution afforded needle crystals of *trans*-3-iodoacrylic acid.[29] Rectangular crystals of **11*Me$_2$** deposited upon slow evaporation of a MeOH solution at ambient temperature, while cooling of a hot MeOH solution resulted in thermal isomerization to **12*Me$_2$**. Fragile plate crystals of deca-4,6-diyne-1,10-dioic acid dimethyl ester were produced by slow evaporation of an ethyl acetate solution. Column-shaped crystals of both **13*Me$_2$** and **14*Me$_2$** were grown by slow cooling of hot MeOH solutions.

Single crystals of $[Mo_2(DAniF)_3(MeCN)_2]BPh_4$, [**1**]$BPh_4$, suitable for X-ray diffraction analysis were grown by vapor diffusion of Bu^tOMe into a saturated MeCN solution. Crystals of $Mo_2(DAniF)_3Cl(MeCN)\cdot 0.5CH_2Cl_2$ (**2**$\cdot 0.5CH_2Cl_2$) grew by diffusion of a 1:25 Et_2O:hexanes mixture into a 12:1 CH_2Cl_2:MeCN solution. Slow introduction of a 1:25 Et_2O:hexanes mixture into CH_2Cl_2 solutions afforded crystalline **3**$\cdot 0.5CH_2Cl_2\cdot 0.5C_6H_{14}$, **4**, and **5**$\cdot 2CH_2Cl_2$. Similarly, crystals of **7**$\cdot ClCH_2CH_2Cl$, **10**$\cdot 2ClCH_2CH_2Cl$, **11**$\cdot 3.5ClCH_2CH_2Cl\cdot Et_2O$, and **12**$\cdot 2ClCH_2CH_2Cl$ were obtained by diffusing an Et_2O/hexanes mixture into $ClCH_2CH_2Cl$ solutions of the respective compounds. Crystals of **13**$\cdot C_7H_8\cdot C_8H_{18}$ were prepared by diffusion of 1:10 toluene:2,2,4-trimethylpentane into a 1,3-dichlorobenzene solution diluted 50% from the point of saturation. A similar approach, but with a 1:10 toluene:hexanes mixture instead of 1:10 toluene:2,2,4-trimethylpentane, yielded fine plate crystals of **14**$\cdot C_6H_4Cl_2\cdot C_6H_{14}$.

X-ray diffraction data for **13*Me$_2$** and for **3**$\cdot 0.5CH_2Cl_2\cdot 0.5C_6H_{14}$ were collected on a Nonius FAST diffractometer utilizing the program MADNES.[32] A suitable crystal was mounted on the tip of a quartz fiber with a small amount of silicone grease and transferred to a goniometer head. Cell parameters were obtained from an autoindexing routine and were refined with 250 reflections within a 2θ range of 18.1−41.6°. The cell dimensions and Laue symmetry were confirmed with axial photographs. The data were corrected for Lorentz and polarization effects and were processed using an ellipsoid−mask algorithm (the program PROCOR).[33] The program SORTAV[34] was used to correct for absorption.

Data for 3-chloro-*cis*-2-pentene dioic acid, *trans*-3-iodoacrylic acid, **5*H**, **11*Me$_2$**, **12*Me$_2$**, deca-4,6-diyne-1,10-dioic acid dimethyl ester, **14*H$_2$**, [**1**]BPh_4, **2**$\cdot 0.5CH_2Cl_2$, **4**, **5**$\cdot 2CH_2Cl_2$, **7**$\cdot ClCH_2CH_2Cl$, **10**$\cdot 2ClCH_2CH_2Cl$, **11**$\cdot 3.5ClCH_2CH_2Cl\cdot Et_2O$, **12**$\cdot 2ClCH_2CH_2Cl$, **13**$\cdot C_7H_8\cdot C_8H_{18}$, and **14**$\cdot C_6H_4Cl_2\cdot C_6H_{14}$ were collected using a Bruker SMART 1000 CCD area detector system with ω scans of 0.3 deg/frame with 30, 60, or 90 s frames such that 1271 frames were collected for a hemisphere of data. The first 50 frames were recollected at the end of the data collection to monitor for crystal decay, but no significant decomposition was observed. Cell parameters were determined using the program SMART,[35] and data reduction and integration were performed with the software package SAINT,[36] which corrects for Lorentz, polarization, and decay effects, while absorption corrections were applied by using the program SADABS.[36]

In all structures, the positions of some or all of the non-hydrogen atoms were found by a direct methods solution using the SHELX[37] software. For all structures, subsequent cycles of least squares refinement followed by difference Fourier syntheses revealed the positions of the remaining non-hydrogen atoms. For all molybdenum containing molecules and for deca-4,6-diyne-1,10-dioic acid dimethyl ester, hydrogen atoms were added in calculated positions and refined isotropically as riding atoms with displacement parameter values of 1.2 times those of the carbon atoms to which they were attached. For texic acid dimethyl ester, the positions of the vinyl hydrogen atoms were refined, while the methyl hydrogen atoms were added in calculated positions and refined as riding atoms. In the remaining organic molecules, the positions of all hydrogen atoms were visible in the final electron density maps and were therefore allowed to refine. Crystallographic data and refinement results are presented as Supporting Information, while selected metrical parameters are collected in Tables 1 and 2 for the molybdenum containing molecules.

Syntheses. A. Tamuic Acid, 13*H$_2$. Octa-*trans,trans,trans*-2,4,6-triene-1,8-dioate dimethyl ester, **13*Me$_2$**, (0.300 g, 1.54 mmol) was suspended in MeOH (10 mL) and treated with an aqueous solution of Et_4NOH (12.6 mL of 35 wt % solution, 12.9 g, 30.6 mmol). The mixture was refluxed for 12 h, and the MeOH was then removed under vacuum. The remaining aqueous solution was acidified with 20 mL of 25% aqueous HCl, which induced precipitation of a cream colored solid. This solid was collected by filtration, washed with 2×5 mL distilled H_2O, and dried under vacuum. Yield: 0.210 g, 82%. The compound was used without further purification. Because of its sparing solubility in organic solvents, tamuic acid was not readily subject to characterization other than the X-ray crystallography of the corresponding dimethyl ester.

B. Texic Acid, 14*H$_2$. As initially prepared by the base catalyzed rearrangement of deca-4:6-diyne-1,10-dioic acid, texic acid was not sufficiently pure for further use. Therefore, purification was accomplished by converting texic acid to its dimethyl ester, **14*Me$_2$**, vacuum subliming it, and recrystallizing it from MeOH. Deprotection of **14*Me$_2$** (0.237 g, 1.07 mmol) was then done in the same manner as described for tamuic acid. Texic acid was isolated as a bright yellow solid. Yield: 0.207 g, 97%.

C. [Mo$_2$(DAniF)$_3$(MeCN)$_2$]BPh$_4$, [1]BPh$_4$. A 100 mL Schlenk flask was charged with a stir bar, $Mo_2(DAniF)_3Cl_2$ (0.251 g, 0.214 mmol), $NaBPh_4$ (0.0835 g, 0.214 mmol), Zn dust (5.0 g), and 50 mL of MeCN. The heterogeneous mixture was stirred for 1 h at ambient temperature. The reaction mixture was filtered through a packed Celite column to remove Zn dust. The light yellow filtrate was concentrated to dryness under vacuum. The resulting yellow solid was redissolved in a minimal volume of MeCN (~3 mL), and Bu^tOMe was added by vapor diffusion over a period of 48 h. The yellow microcrystalline precipitate was collected by filtration, washed successively with 5 mL portions of 33%

(32) Pflugrath, J.; Messerschmitt, A. *MADNES, Munich Area Detector (New EEC) System*, version EEC 11/1/89; with enhancements by Nonius Corporation: Delft, The Netherlands. A description of MADNES appears in the following: Messerschmitt, A.; Pflugrath, J. *J. Appl. Crystallogr.* **1987**, *20*, 306.
(33) (a) Kabsch, W. *J. Appl. Crystallogr.* **1988**, *21*, 67. (b) Kabsch, W. *J. Appl. Crystallogr.* **1988**, *21*, 916.
(34) Blessing, R. H. *Acta Crystallogr.* **1995**, *A51*, 33.
(35) *SMART for Windows NT*, version 5.059; Bruker Analytical X-ray Systems; 1997−1998.
(36) *SAINT+ for NT*, version 6.02; Bruker Analytical X-ray Systems; 1997−1999.
(37) Sheldrick, G. M. *SHELX-97 Programs for Crystal Structure Analysis*. Institüt für Anorganische Chemie der Universität: Tammanstrasse 4, D-3400 Göttingen, Germany, 1998.

Table 1. Selected Interatomic Distances (Å) for Compounds **1**−**5**, **7**, **10**−**14**

	1	**2**	**3**[a]	**4**	**5**	**7**	**10**	**11**	**12**	**13**	**14**
d,[b] Å						7.693	9.395	10.350	11.575	13.920	16.156
Mo(1)−Mo(2)	2.1079(5)	2.111(6)	2.091(1)	2.0884(3)	2.0899(3)	2.0900(3)	2.0919(3)	2.087(1)	2.0869(4)	2.0862(8)	2.0898(6)
Mo(3)−Mo(4)						2.0928(3)		2.0873(9)			
Mo(1)−X(1)[c]	2.200(4)	2.468(1)	2.147(5)	2.147(2)	2.125(2)	2.092(2)	2.140(2)	2.146(5)	2.128(2)	2.149(4)	2.119(3)
Mo(2)−X(2)[c]	2.184(4)	2.169(5)	2.150(6)	2.152(2)	2.130(2)	2.164(2)	2.149(2)	2.119(5)	2.141(2)	2.128(4)	2.149(3)
Mo(3)−O(3)						2.099(2)		2.133(5)			
Mo(4)−O(4)						2.172(2)		2.121(6)			
Mo(1)−N(1)	2.155(4)	2.149(4)	2.152(6)	2.136(2)	2.152(2)	2.137(2)	2.144(2)	2.165(7)	2.158(3)	2.151(5)	2.131(5)
Mo(1)−N(3)	2.080(4)	2.121(4)	2.112(6)	2.132(2)	2.116(3)	2.133(2)	2.108(2)	2.126(6)	2.128(3)	2.127(5)	2.127(4)
Mo(1)−N(5)	2.149(4)	2.192(4)	2.153(7)	2.144(2)	2.133(2)	2.153(2)	2.144(2)	2.163(7)	2.160(3)	2.155(5)	2.146(5)
Mo(2)−N(2)	2.125(4)	2.138(4)	2.145(7)	2.161(2)	2.158(2)	2.134(2)	2.167(2)	2.139(7)	2.138(3)	2.161(5)	2.154(4)
Mo(2)−N(4)	2.119(4)	2.121(4)	2.131(6)	2.134(2)	2.137(2)	2.146(2)	2.153(2)	2.127(6)	2.142(3)	2.132(5)	2.123(4)
Mo(2)−N(6)	2.142(4)	2.152(4)	2.142(7)	2.158(2)	2.153(2)	2.135(2)	2.129(2)	2.142(7)	2.148(3)	2.132(5)	2.150(4)
Mo(3)−N(7)						2.177(3)		2.155(6)			
Mo(3)−N(9)						2.121(3)		2.138(6)			
Mo(3)−N(11)						2.151(3)		2.144(7)			
Mo(4)−N(8)						2.136(2)		2.146(7)			
Mo(4)−N(10)						2.130(2)		2.131(7)			
Mo(4)−N(12)						2.127(2)		2.129(7)			
Selected Bond Distances for Carboxylate Ligand or MeCN Ligands											
					C(2)−C(3) 1.330(5)		C(1)−C(2) 1.483(4)	C(3)−C(5) 1.33(1)	C(1)−C(2) 1.471(4)	C(2)−C(3) 1.331(9)	C(2)−C(3) 1.329(7)
	N(7)−C(46) 1.106(6)	N(7)−C(46) 1.126(7)	C(1)−C(2) 1.44(1)	C(1)−C(2) 1.487(3)	C(3)−C(4) 1.451(5)	C(3)−C(4) 1.327(4)	C(2)−C(3) 1.305(2)	C(4)−C(6) 1.34(1)	C(2)−C(3) 1.337(4)	C(4)−C(4A) 1.34(1)	C(4)−C(5) 1.345(8)
	N(8)−C(48) 1.138(6)		C(2)−C(3) 1.18(1)	C(2)−C(3) 1.307(4)	C(4)−C(5) 1.329(6)		C(3)−C(2A) 1.305(2)	C(5)−C(6) 1.45(1)	C(3)−C(3A) 1.449(6)	C(3)−C(4) 1.436(9)	C(5)−C(5A) 1.40(1)

[a] Values are for one of two molecules in the asymmetric unit; values for the other one are very similar. [b] d = distance between centroids of the two Mo_2 units. [c] X(1), X(2) = N(7), N(8) for **1**; Cl(1), N(2) for **2**; O(1), O(2) for **3**−**5**, **7**, **10**−**14**.

MeCN in Bu^{t}OMe, 20% MeCN in Bu^{t}OMe, Bu^{t}OMe, and Et_2O, and dried under vacuum. Yield: 0.193 g, 58%. ^{1}H NMR δ (ppm in CD_3CN) 8.89 (s, 2H, −NC*H*N−), 8.29 (s, 1H, −NC*H*N−), 7.27 (m, 8H, aromatic C−H), 6.99 (t, 8H, aromatic C−H), 6.85 (d, 4H, aromatic C−H), 6.57−6.73 (m, 16H, aromatic C−H), 6.43 (d, 4H, aromatic C−H), 6.12 (d, 4H, aromatic C−H), 3.71 (s, 12 H, −OCH_3), 3.61 (s, 6 H, −OCH_3), 1.96 (s, 6H, CH_3CN).

D. Mo_2(DAniF)$_3$Cl(MeCN) (2). A solution of $Mo_2(DAniF)_3Cl_2$ (0.500 g, 0.486 mmol) in MeCN was stirred over Zn dust (5 g) for 2 h. The resulting yellow solution was filtered into a 5 mL solution of $BzEt_3NCl$ (0.111 g, 0.486 mmol) in MeCN. This mixture was stirred for several hours and became somewhat turbid. The solvent was removed under vacuum, and the resulting residue was stirred vigorously overnight with 5 mL of fresh MeCN. The fine yellow-orange powder that developed was isolated by filtration and washed with an additional 2 mL portion of MeCN. The remaining solid was extracted with 3 × 2 mL of CH_2Cl_2 and filtered into a clean Schlenk tube. The filtrate was then diluted with 0.5 mL of MeCN and layered with Et_2O (3 mL) followed by hexanes (40 mL). After 4 days, large yellow needle crystals (0.256 g, 49% yield) were collected by filtration. ^{1}H NMR δ (ppm in 1:1 CD_2Cl_2:CD_3CN) 8.74 (s, 2H, −NC*H*N−), 8.25 (s, 1H, −NC*H*N−), 6.85 (d, 4H, aromatic C−H), 6.58−6.67 (dd, 8H, aromatic C−H), 6.49 (d, 4H, aromatic C−H), 6.40 (d, 2H, aromatic C−H), 6.28 (d, 2H, aromatic C−H), 6.14 (d, 2H, aromatic C−H), 5.93 (d, 2H, aromatic C−H), 3.70 (s, 6 H, −OCH_3), 3.68 (s, 6H, −OCH_3), 3.62 (s, 3H, −OCH_3), 3.57 (s, 3H, −OCH_3), 2.00 (s, 3H, NCCH_3). Absorption spectrum (CH_2Cl_2) λ_{max} (ϵ_M): 479 (1220). Anal. Calcd for [Mo_2(DAniF)$_3$Cl(MeCN)]·0.25(CH_2Cl_2), $C_{47.25}H_{48.5}Cl_{1.5}Mo_2N_7O_6$: C, 53.77; H, 4.63; N, 9.29. Found: C, 53.88; H, 4.60; N, 9.21.

E. Mo_2(DAniF)$_3$(O_2CX) Compounds. The procedure used was that of Method B in ref 23.

F. Mo_2(DAniF)$_3$(O_2CC≡CH) (3). 1 equiv of $(Et_4N)_2(O_2CC{\equiv}CCO_2)$ was used rather than the corresponding propiolate salt, and the crude product was washed with H_2O (2 × 10 mL) followed by Et_2O (5 mL). Propiolate formed in situ from a spontaneous decarboxylation of acetylene dicarboxylate when an excess of the latter was used. Yield: 48%. ^{1}H NMR δ (ppm in CD_2Cl_2) 8.54 (s, 2H, −NC*H*N−), 8.43 (s, 1H, −NC*H*N−), 6.68 (d, 8H, aromatic C−H), 6.53 (d, 8H, aromatic C−H), 6.44 (d, 4H, aromatic C−H), 6.21 (d, 4H, aromatic C−H), 3.72 (s, 12 H, −OCH_3), 3.63 (s, 6H, −OCH_3), 2.86 (s, 1H, −C≡C−*H*). Absorption spectrum (CH_2Cl_2) $_{max}$ (ϵ_M): 265 (55 400), 301 (59 000), 435 (sh). Anal. Calcd for $C_{48}H_{46}Mo_2N_6O_8$: C, 56.15; H, 4.52; N, 8.18. Found: C, 55.61; H, 4.31; N, 8.05.

G. Mo_2(DAniF)$_3$(O_2CH=CH_2) (4). Yield: 72%. ^{1}H NMR δ (ppm in CD_2Cl_2): 8.47 (s, 2H, −NC*H*N−), 8.45 (s, 1H, −NC*H*N−), 6.65 (d, 8H, aromatic C−H), 6.53 (d, 8H, aromatic C−H), 6.44 (d, 4H, aromatic C−H), 6.38 (dd, 1H, vinyl C−H), 6.22 (d, 4H, aromatic C−H), 5.76 (dd, 1H, vinyl C−H), 3.71 (s, 12H, −OCH_3), 3.63 (s, 6H, −OCH_3). The remaining vinyl hydrogen atom of the acrylate ligand was obscured by aromatic C−H resonances. Absorption spectrum (CH_2Cl_2) λ_{max} (ϵ_M): 268 (49 500), 301 (52 700), 405 (sh), 445 (sh). Anal. Calcd for $C_{48}H_{48}Mo_2N_6O_8$: C, 56.04; H, 4.70; N, 8.17. Found: C, 56.22; H, 4.75; N, 8.24.

H. Mo_2(DAniF)$_3$((*E*)-O_2CCH=CH−CH=CH_2) (5). Yield: 35%. ^{1}H NMR δ (ppm in CD_2Cl_2): 8.47 (s, 2H, −NC*H*N−), 8.46 (s, 1H, −NC*H*N−), 7.36 (dd, 1H, vinyl C−H), 7.11 (br, 1H, vinyl C−H), 6.86 (br, 1H, vinyl C−H), 6.66 (d, 8H, aromatic C−H), 6.53 (d, 8H, aromatic C−H), 6.44 (d, 4H, aromatic C−H), 6.23 (d, 4H, aromatic C−H), 5.37−5.61 (m, 1H, vinyl C−H), 3.71 (s, 12H, −OCH_3), 3.64 (s, 6H, −OCH_3). The remaining vinyl hydrogen atom of the (*E*)-penta-2,4-dienoate ligand was obscured by aromatic C−H resonances. Absorption spectrum (CH_2Cl_2) λ_{max} (ϵ_M): 253 (73 000), 301 (59 400), 454 (7750). Anal. Calcd for [Mo_2(DAniF)$_3$((*E*)-O_2CCH=CH−CH=CH_2)]·CH_2Cl_2, $C_{51}H_{52}Cl_2Mo_2N_6O_8$: C, 53.74; H, 4.60; N, 7.37. Found: C, 53.47; H, 4.69; N, 7.50.

H. [Mo_2(DAniF)$_3$]$_2$(μ-O_2C−X−CO_2) Compounds. The procedure used was that of Method B in ref 23 but with $[Mo_2(DAniF)_3(MeCN)_2]^+$ introduced to the dicarboxylate salt in the stoichiometric ratio of 2:1.

I. [Mo_2(DAniF)$_3$]$_2$(μ-maleate) (7). Yield: 52%. ^{1}H NMR δ (ppm in CD_2Cl_2): 8.47 (s, 2H, −NC*H*N−), 8.37 (s, 4H, −NC*H*N−), 6.67 (s, 2H, vinyl C−H), 6.53 (d, 16H, aromatic C−H), 6.39 (d, 8H, aromatic C−H), 6.34 (d, 16H, aromatic C−H), 6.08 (d, 8H, aromatic C−H), 3.62 (s, 12H, −OCH_3), 3.56 (s, 24H, −OCH_3). Absorption spectrum (CH_2Cl_2) λ_{max} (ϵ_M): 265 (106 000), 298 (106 000), 519 (11 700). Anal. Calcd for [Mo_2(DAniF)$_3$]$_2$(μ-maleate)·$ClCH_2CH_2Cl$, $C_{96}H_{96}Cl_2Mo_4N_{12}O_{16}$: C, 54.17; H, 4.55; N, 7.90. Found: C, 54.13; H, 4.73; N, 7.94.

Table 2. Selected Angles (deg) for Compounds **1**−**5**, **7**, **10**−**14**

	1	**2**	**3**[a]	**4**	**5**	**7**	**10**	**11**	**12**	**13**	**14**
ϕ,[b] deg						42.9	62.9	11.1	0	0	0
X(1)−Mo(1)−N(1)[c]	86.3(2)	84.7(1)	87.3(2)	86.67(6)	89.49(9)	88.30(9)	86.80(8)	88.3(2)	87.81(9)	89.9(2)	85.6(2)
X(1)−Mo(1)−N(3)[c]	162.0(1)	158.0(1)	174.1(2)	174.69(6)	174.51(8)	173.10(9)	175.0(8)	176.1(2)	174.0(1)	175.4(2)	174.8(2)
X(1)−Mo(1)−N(5)[c]	88.9(2)	91.6(1)	87.8(2)	88.18(6)	84.30(9)	85.63(9)	89.00(8)	85.3(2)	87.85(9)	87.1(2)	86.4(2)
X(2)−Mo(2)−N(2)[c]	83.5(1)	89.7(2)	87.0(2)	86.50(6)	88.89(9)	90.91(8)	86.57(8)	87.7(2)	87.71(9)	88.2(2)	86.4(2)
X(2)−Mo(2)−N(4)[c]	168.3(1)	164.2(2)	176.7(2)	175.11(6)	175.07(8)	175.85(8)	175.03(7)	175.1(2)	175.1(1)	174.4(2)	175.2(1)
X(2)−Mo(2)−N(6)[c]	91.0(1)	82.7(20	87.9(3)	88.48(6)	84.87(9)	87.05(8)	88.47(8)	84.6(2)	87.31(9)	86.3(2)	88.2(2)
O(3)−Mo(3)−N(7)						84.28(9)		87.8(2)			
O(3)−Mo(3)−N(9)						174.03(9)		175.9(2)			
O(3)−Mo(3)−N(11)						87.76(9)		86.5(2)			
O(4)−Mo(4)−N(8)						84.17(9)		87.8(2)			
O(4)−Mo(4)−N(10)						175.99(9)		174.4(2)			
O(4)−Mo(4)−N(12)						90.09(9)		86.8(2)			
N(1)−Mo(1)−N(5)	174.3(1)	175.9(2)	173.6(2)	172.06(7)	171.76(9)	172.6(1)	173.26(9)	172.0(3)	173.1(1)	173.7(2)	170.1(2)
N(2)−Mo(2)−N(6)	172.7(1)	170.7(2)	171.8(3)	173.13(6)	171.70(9)	173.84(9)	172.93(8)	170.3(3)	172.6(1)	175.5(2)	173.0(2)
N(7)−Mo(3)−N(11)						171.1(1)		176.6(3)			
N(8)−Mo(4)−N(12)						171.43(9)		172.1(3)			
Selected Bond Angles for Carboxylate Ligand and MeCN Ligands											
											C(1)−C(2)−C(3) 122.6(5)
	N(7)−C(46)−C(47) 179.5(7)	N(7)−C(46)−C(47) 177.1(7)	C(1)−C(2)−C(3) 176(1)	C(1)−C(2)−C(3) 123.3(3)	C(1)−C(2)−C(3) 123.1(3)	C(1)−C(3)−C(4) 133.2(3)	C(20−C(3)−C(2A) 174.8(5)	C(3)−C(5)−C(6) 126.6(9)	C(2)−C(3)−C(3A) 124.594)	C(2)−C(3)−C(4) 126.0(7)	C(2)−C(3)−C(4) 126.6(6)
	N(8)−C(48)−C(49) 178.6(6)				C(2)−C(3)−C(4) 124.6(3)	C(2)−C(4)−C(3) 133.7(3)	C(1)−C(2)−C(3) 124.3(3)	C(4)−C(6)−C(5) 128.2(9)	C(1)−C(2)−C(3) 123.2(3)	C(3)−C(4)−C(4A) 123.5(9)	C(3)−C(4)−C(5) 124.0(6)
					C(3)−C(4)−C(5) 123.7(4)					C(1)−C(2)−C(3) 123.8(6)	C(4)−C(5)−C(5A) 125.3(8)

[a] Values are for one of two molecules in the asymmetric unit. [b] ϕ = twist angle between Mo_2 axes. [c] X(1) = N(7), X(2) = N(8) for **1**; X(1) = Cl(1), X(2) = N(7) for **2**; X(1) = O(1), X(2) = O(2) for **3**−**5**, **7**, **10**−**14**.

J. $[Mo_2(DAniF)_3]_2$(μ-glutinate) (10). Yield: 49%. ^{1}H NMR δ (ppm in CD_2Cl_2): 8.43 (s, 2H, −NC*H*N−), 8.41 (s, 4H, −NC*H*N−), 6.79 (s, 2H, C═C(*H*)CO_2), 6.48−6.66 (m, 32H, aromatic C−H), 6.40 (d, 8H, aromatic C−H), 6.15 (d, 8H, aromatic C−H), 3.69 (s, 12H, −OCH_3), 3.62 (s, 12H, −OCH_3), 3.61 (s, 12H, −OCH_3). Absorption spectrum (CH_2Cl_2) λ_{max} (ϵ_M): 288 (92 500), 315 (sh), 435 (sh). Anal. Calcd for $C_{95}H_{92}Mo_4N_{12}O_{16}$: C, 55.89; H, 4.54; N, 8.23. Found: C, 55.60; H, 4.53; N, 8.13.

K. $[Mo_2(DAniF)_3]_2$(μ-*cis,cis*-muconate) (11). Yield: 74%. ^{1}H NMR (δ in CD_2Cl_2): 8.49 (s, 2H, −NC*H*N−), 8.47 (s, 4H, −NC*H*N−), 8.04 (dd, 2H, vinyl C−H), 6.65 (d, 16H, aromatic C−H), 6.53 (d, 16H, aromatic C−H), 6.44 (d, 8H, aromatic C−H), 6.31 (d, 1H, vinyl C−H), 6.23 (d, 8H, aromatic C−H), 3.70 (s, 24H, −OCH_3), 3.64 (s, 12H, −OCH_3). The remaining vinyl hydrogen atom of the *cis,cis*-muconate bridge was obscured by aromatic C−H resonances. Absorption spectrum (CH_2Cl_2) λ_{max} (ϵ_M): 266 (125 000), 293 (119 000), 546 (13 400). Anal. Calcd for $C_{96}H_{94}Mo_4N_{12}O_{16}$: C, 56.09; H, 4.61; N, 8.18. Found: C, 56.03; H, 4.53; N, 8.06.

L. $[Mo_2(DAniF)_3]_2$(μ-*trans,trans*-muconate) (12). Yield: 64%. ^{1}H NMR δ (ppm in CD_2Cl_2): 8.47 (s, 2H, −NC*H*N−), 8.45 (s, 4H, −NC*H*N−), 7.52 (dd, 2H, vinyl C−H), 6.65 (d, 16H, aromatic C−H), 6.62 (dd, 2H, vinyl C−H), 6.53 (d, 16H, aromatic C−H), 6.44 (d, 8H, aromatic C−H), 6.22 (d, 8H, aromatic C−H), 3.70 (s, 24H, −OCH_3), 3.64 (s, 12H, −OCH_3). Absorption spectrum (CH_2Cl_2) λ_{max} (ϵ_M): 268 (117 000), 293 (sh), 566 (16 100). Anal. Calcd for $[Mo_2(DAniF)_3]_2$(μ-*trans,trans*-muconate)·3$ClCH_2CH_2Cl$, $C_{102}H_{106}Cl_6Mo_4N_{12}O_{16}$: C, 52.08; H, 4.54; N, 7.14. Found: C, 52.01; H, 4.55; N, 7.34.

M. $[Mo_2(DAniF)_3]_2$(μ-tamuate) (13). Yield: 57%. ^{1}H NMR δ (ppm in CD_2Cl_2): 8.47 (s, 6H, −NC*H*N−), 7.39−7.51 (m, 2H, vinyl C−H), 7.08 (br, 1H, vinyl C−H), 6.87 (br, 1H, vinyl C−H), 6.76 (dd, 2H, vinyl C−H), 6.66 (d, 16H, aromatic C−H), 6.53 (d, 16H, aromatic C−H), 6.44 (d, 8H, aromatic C−H), 6.22 (d, 8H, aromatic C−H), 3.71 (s, 24H, −OCH_3), 3.64 (s, 12H, −OCH_3). Absorption spectrum (CH_2Cl_2) λ_{max} (ϵ_M): 305 (128 000), 581 (18 100). Anal. Calcd for $C_{98}H_{96}Mo_4N_{12}O_{16}$: C, 56.54; H, 4.65; N, 8.07. Found: C, 55.75; H, 4.68; N, 7.93.

N. $[Mo_2(DAniF)_3]_2$(μ-texate) (14). Yield: 73%. ^{1}H NMR δ (ppm in CD_2Cl_2): 8.46 (s, 6H, −NC*H*N−), 7.42 (dd, 2H, vinyl C−H), 7.07 (br, 2H, vinyl C−H), 6.85 (br, 2H, vinyl C−H), 6.66 (d, 16H, aromatic C−H), 6.53 (d, 16H, aromatic C−H), 6.44 (d, 8H, aromatic C−H), 6.39 (d, 2H, vinyl C−H), 6.22 (d, 8H, aromatic C−H), 3.71 (s, 24H, −OCH_3), 3.64 (s, 12H, −OCH_3). Absorption spectrum (CH_2Cl_2) λ_{max} (ϵ_M): 251 (75 000), 308 (99 400), 329 (102 000), 588 (19 300). Anal. Calcd for $C_{100}H_{98}Mo_4N_{12}O_{16}$: C, 56.99; H, 4.69; N, 7.97. Found: C, 56.67; H, 4.77; N, 7.97.

O. $[Mo_2(DAniF)_3]_2$(μ-terephthalate) (15).[38] Yield: 79%. ^{1}H NMR δ (ppm in CD_2Cl_2): 8.51 (s, 2H, −NC*H*N−), 8.45 (s, 4H, −NC*H*N−), 8.40 (s, 4H, aromatic C−H), 6.67 (d, 16H, aromatic C−H), 6.59 (d, 16H, aromatic C−H), 6.47 (d, 8H, aromatic C−H), 6.26 (d, 8H, aromatic C−H), 3.71 (s, 24H, −OCH_3), 3.65 (s, 12H, −OCH_3). Absorption spectrum (CH_2Cl_2) λ_{max} (ϵ_M): 252 (98 400), 299 (93 900), 492 (15 200). Anal. Calcd for $C_{98}H_{94}Mo_4N_{12}O_{16}$: C, 56.60; H, 4.56; N, 8.08. Found: C, 56.38; H, 4.40; N, 8.11.

Results and Discussion

Syntheses and Structures of Organic Ligands. Several of the mono- and dicarboxylic acids of interest (**5*H**, **10*H$_2$**, **13*H$_2$**, and **14*H$_2$**) were unavailable commercially but were accessible in usable quantities according to literature methods. These syntheses are collectively summarized in Figure 1, where displacement ellipsoid drawings are used to indicate those compounds that have been characterized by X-ray crystallography. This was essential because the original preparations of some of these molecules were accompanied by incomplete physical characterization and there was a need to confirm their identities and also to provide a comparison for key metric parameters between the free organic molecules and coordinated mono- and dicarboxylates.

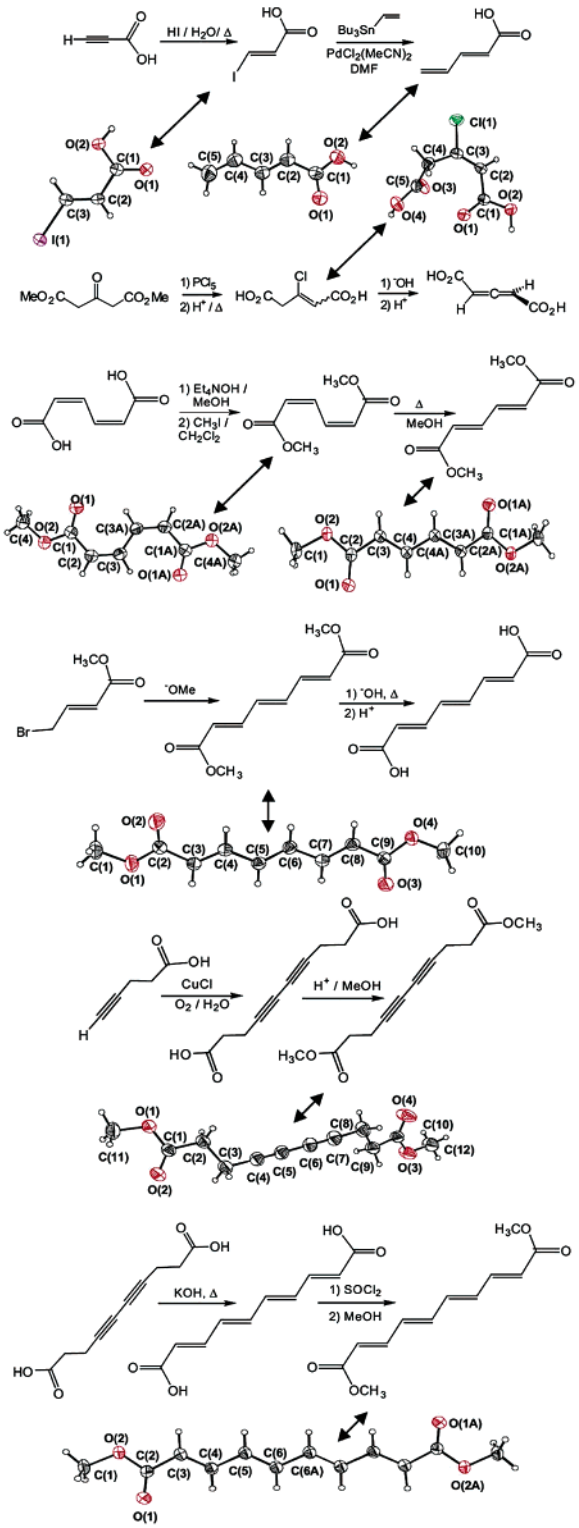

Figure 1. Preparations of **5*H**, **10*H$_2$**, **11*Me$_2$**, **12*Me$_2$**, **13*H$_2$**, and **14*H$_2$**. Thermal ellipsoid plots are drawn at the 50% probability level. The double ended arrows relate the line drawings to their corresponding thermal ellipsoid plots.

(38) The crystal structure of **15**·2C_6H_{14} has been reported: Cotton, F. A.; Donahue, J. P.; Lin, C.; Murillo, C. A.; Rockwell, J. *Acta Crystallogr.* **2002**, *E58*, m298.

Table 3. Comparison of Carbon−Carbon Bond Lengths in the Polyolefinic Compounds $Me_2OC(CH{=}CH)_nCO_2Me$ and $[Mo_2(DAniF)_3](O_2C(CH{=}CH)_nCO_2)[Mo_2(DAniF)_3]$ ($n = 2-4$)[a]

compound	$(C-C)_{av}$,[b,c] Å	$(C{=}C)_{av}$,[b] Å	Δ,[b,d] Å
$MeO_2C(CH{=}CH)_2CO_2Me$	1.450(2)[e]	1.333(2)[e]	0.117(4)
$MeO_2C(CH{=}CH)_3CO_2Me$	1.437(2)	1.332(2)	0.105(3)
$MeO_2C(CH{=}CH)_4CO_2Me$	1.445(1)	1.342(1)	0.103(2)
$[Mo_2(DAniF)_3](O_2C(CH{=}CH)_2CO_2)[Mo_2(DAniF)_3]$	1.449(6)[e]	1.337(4)[e]	0.11(1)
$[Mo_2(DAniF)_3](O_2C(CH{=}CH)_3CO_2)[Mo_2(DAniF)_3]$	1.436(9)[e]	1.336(7)	0.10(1)
$[Mo_2(DAniF)_3](O_2C(CH{=}CH)_4CO_2)[Mo_2(DAniF)_3]$	1.416(6)	1.337(5)	0.079(8)

[a] All double bonds have the *trans* configuration. With the exception of $Me_2OC(CH{=}CH)_3CO_2Me$, all molecules in the table crystallized on an inversion center. Only those C−C and C=C bond distances which were crystallographically independent were used in determining $(C-C)_{av}$, $(C{=}C)_{av}$, and Δ. [b] Error propagations were determined using the general formula for uncertainty in a function of several variables as detailed in ref 45, pp 73−77. [c] The carbon−carbon single bond α to the carbonyl carbon, $O_2C-(CH{=}CH)_n$, was not included in this calculation. [d] $\Delta = (C-C)_{av} - (C{=}C)_{av}$. [e] These values are not averages, since only one bond distance was available.

A few general remarks on the syntheses and characterization of the organic compounds used as precursors to the ligands are relevant to anyone trying to duplicate these syntheses. The compound 3-chloro-2-pentenedioic acid was readily prepared, not in a pure form but as a 2:1 mixture of the corresponding *cis* and *trans* isomers, as determined by ^{1}H NMR.[39] The *cis* isomer crystallizes by evaporation of an Et_2O solution and orders itself into a herringbone type of end-to-end H-bonded pattern. The diacid **10*H$_2$** was formed in good yield as a mixture of enantiomers upon treatment of 3-chloro-2-pentenedioic acid with aqueous base.[27] The acid **5*H** was obtained by the Pd(II) mediated Stille coupling between tributyl vinyl tin and *trans*-3-iodoacrylic acid.[29] The latter molecule was readily prepared by the addition of HI to propiolic acid and, like **5*H** itself, readily crystallized from Et_2O and was further identified by an X-ray crystal structure. Unit cell parameters and refinement results for all organic compounds are available as Supporting Information.

For **13*H$_2$**, the corresponding dimethyl ester was obtained by the self-condensation of methyl-4-bromocrotonate in $NaOCH_3$/C_6H_6.[28] The diacid was then obtained in good yield by deprotection in aqueous base. The next member in the series of polyolefinic α,ω-dicarboxylic acids, **14*H$_2$**, was prepared by a base-catalyzed prototropic shift rearrangement of deca-4,6-diyne-1,10-dioic acid.[30] The material thus obtained requires a further degree of purification by transformation to the dimethyl ester, vacuum sublimation, and recrystallization from MeOH. Deca-4,6-diyne-1,10-dioic acid was accessible by CuCl mediated coupling of commercially available 4-pentynoic acid[31] and was structurally characterized as its dimethyl ester. Although higher polyolefinic α,ω-dicarboxylic acids, with five, six, and seven conjugated carbon−carbon double bonds in an all-*trans* configuration are known in the chemical literature,[40] their syntheses require rather inaccessible starting materials and hence an exponentially greater amount of work. Thus, these acids have not yet been prepared by us, but they will be the target of future studies.

The scant organic literature which can be found concerning **13*H$_2$** and **14*H$_2$** or their dimethyl esters deals only with their preparation and isolation. Inasmuch as we appear to be the first to have found some further use for these molecules, we have resorted to designating them by the more convenient, nonsystematic names tamuic acid and texic acid, respectively. Since both tamuic and texic acid are only sparingly soluble in organic solvents, they were more effectively purified and characterized as the corresponding dimethyl esters. Both dimethyl esters were characterized crystallographically (Figure 1) and reveal a linear chain of alternating single and double bonds (Table S4, Supporting Information). Texic acid dimethyl ester is fully 16 Å from end to end and crystallizes parallel to the *c* axis on an inversion center in the space group $P\bar{1}$. Interestingly, the unit cell for this molecule is comprised of two separate half molecules of the dimethyl ester, with the result that the *c* axis, the longest cell axis, is half the length of the full molecule. It is known that even in infinitely long or large cyclic conjugated polyolefins (the former being commonly called polyacetylenes) the alternating carbon to carbon bonds have long (∼1.44 Å) and short (1.36 Å) distances.[41] In the dimethyl esters of tamuic and texic acids, the differences are somewhat larger than this (Table 3).

Syntheses and Structures of Compounds Containing Mo$_2$ Units. Our common starting material for the preparation of dicarboxylate linked pairs of Mo_2 units $[Mo_2(DAniF)_3]O_2CXCO_2[Mo_2(DAniF)_3]$ has been the mixed-valent species $Mo_2(DAniF)_3Cl_2$.[25] In the presence of Zn dust in MeCN, dark brown $Mo_2(DAniF)_3Cl_2$ is readily reduced to yellow $[Mo_2(DAniF)_3(MeCN)_2]^+$, according to the stoichiometry of the following equation:

$$2Mo_2(DAniF)_3Cl_2 + Zn + 4MeCN \rightarrow 2Mo_2(DAniF)_3(MeCN)_2^{+} + ZnCl_4^{2-}$$

Both the air sensitivity and the high solubility of this cation have rendered it expedient to use it in situ rather than as an isolated and purified material. However, diffraction quality crystals having cation **1** were grown as the BPh_4^- salt, the core structure of which is presented in Figure 2. The isolation and characterization of this salt completes[42] the five-membered series $[Mo_2(DAniF)_n(MeCN)_{(8-2n)}]^{(4-n)+}$, the other members of which have been described in prior work.[43] The $\delta \rightarrow \delta^*$ transition for **1** occurs at 481 nm, consistent with the observed trend toward higher energy as the number of formamidinate ligands increases. As *n* increases from 0 to 4, the corresponding $\delta \rightarrow \delta^*$ transition

(39) The ^{1}H NMR spectrum of the *cis* isomer of 3-chloro-2-pentenedioic acid (d_6-DMSO) was obtained using single crystals from the same set used to determine the crystal structure: 12.86 (br, 2H, $-CO_2H$), 6.23 (s, 1H, vinyl C−H), 3.99 (s, 2H, $-CH_2$).

(40) (a) Kuhn, R.; Grundmann, C. *Chem. Ber.* **1936**, *69*, 1979. (b) Kuhn, R.; Grundmann, C. *Chem. Ber.* **1937**, *70*, 1318. (c) Shaw, B. L.; Whiting, M. C. *J. Chem. Soc.* **1954**, 3217.

(41) (a) Longuet-Higgins, H. C.; Salem, L. *Proc. R. Soc. London* **1959**, *A251*, 172. (b) Yannoni, C. S.; Clarke, T. C. *Phys. Rev. Lett.* **1983**, *51*, 1191. (c) Guo, H.; Paldus, J. *Int. J. Quantum Chem.* **1997**, *63*, 345.

(42) For $n = 2$, both *cis* and *trans* isomers are possible, but only the *cis* isomer has proven sufficiently stable to be isolated and studied.

(43) Chisholm, M. H.; Cotton, F. A.; Daniels, L. M.; Folting, K.; Huffman, J. C.; Iyer, S. S.; Lin, C.; Macintosh, A. M.; Murillo, C. A. *J. Chem. Soc., Dalton Trans.* **1999**, 1387.

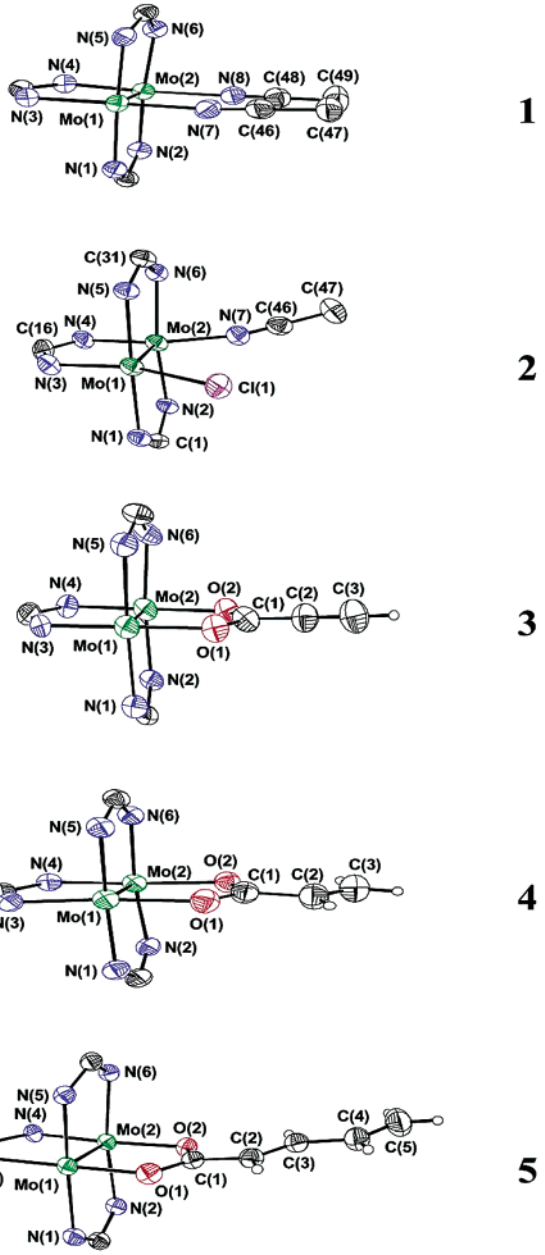

Figure 2. Core structures of the unbridged molecules containing the $Mo_2(DAniF)_3$ unit: $[Mo_2(DAniF)_3(MeCN)_2]^+$, **1**; $Mo_2(DAniF)_3Cl(MeCN)$, **2**; $Mo_2(DAniF)_3(O_2CC{\equiv}CH)$, **3**; $Mo_2(DAniF)_3(O_2CCH{=}CH_2)$, **4**; $Mo_2(DAniF)_3((E)\text{-}(O_2CCH{=}CH{-}CH{=}CH_2))$, **5**. Ellipsoids are drawn at the 50% probability level, and all *p*-anisyl groups are omitted for clarity. Hydrogen atoms are included in the carboxylate ligands to emphasize the stereochemistry.

appears at 597, 570, 516, 481, and 430 nm in keeping with the decreasing Mo−Mo distance and hence increasing δ interaction.

When a soluble source of Cl^-, such as $BzEt_3NCl$, is used in lieu of a bridging dicarboxylate, the asymmetric molecule $Mo_2(DAniF)_3Cl(MeCN)$, **2**, may be isolated in the form of large yellow needle crystals. The core structure of this molecule is presented in Figure 2 and reveals rather appreciable deviations from the bond angles of ∼90° and ∼180° typically observed in tetragonal paddlewheel compounds of this type. For example, the Mo2−Mo1−Cl1 and Mo1−Mo2−N7 bond angles are 108.86(4)° and 103.1(1)°, respectively (Table 2). In the crystalline state, **2** is sufficiently stable for it to be handled briefly in air (tens of minutes) without visible decomposition. Highly soluble in CH_2Cl_2 and THF, this molecule may be useful as an alternative source of the $[Mo_2(DAniF)_3(MeCN)_2]^+$ cation in applications which may require a very precise stoichiometric control or the use of a solvent other than MeCN.

In the course of our first efforts to prepare $[Mo_2(DAniF)_3]_2(\mu\text{-}O_2C{-}C{\equiv}C{-}CO_2)$, we noted that when acetylene dicarboxylate was used in excess of the calculated stoichiometry, it was prone to a decarboxylation reaction which yielded $Mo_2(DAniF)_3(O_2CC{\equiv}CH)$, **3**, as the only identifiable product. The origin of the terminal acetylenic proton is not clear, but the possibility of its being due to adventitious H_2O cannot be ruled out, as the $(Et_4N)_2(O_2CC{\equiv}CCO_2)$ salt is difficult to dry without inducing decomposition. Decarboxylation of acetylene dicarboxylic acid has been noted in other systems[44] and appears to be a quite facile process. Since **3** was of interest in its own right as a comparison to the bridged molecule $[Mo_2(DAniF)_3]_2(\mu\text{-}O_2C{-}C{\equiv}C{-}CO_2)$, it was subjected to a complete characterization. Similarly, the mixed-ligand molecules $Mo_2(DAniF)_3(O_2CCH{=}CH_2)$, **4**, and $Mo_2(DAniF)_3((E)\text{-}O_2CCH{=}CH{-}CH{=}CH_2)$, **5**, were deliberately prepared. The core structures of these molecules are set forth in Figure 2.

Compounds **3**−**5** belong to a family of compounds in which the quadruply bonded Mo_2^{4+} unit is spanned by three formamidinate ligands and a carboxylate anion, thereby forming an unsymmetrical paddlewheel complex. This lowered symmetry is manifest in the ^1H NMR spectra, where two distinct signals in the ratio of 2:1 are observed for the methine protons of the three formamidinate ligands. The weaker *trans* influence of the carboxylate ligand in **3**−**5** is evident by the slightly upfield shift of the methine signal for the formamidinate *trans* to the carboxylate (8.43 ppm for **3**) compared to the formamidinate ligands *cis* to the carboxylate (8.54 ppm for **3**). The Mo−Mo distances fall within a narrow range and are close to 2.09 Å. These distances are slightly shorter than the values of ∼2.11 Å observed for the cation **1** and molecule **2**. The lesser *trans* influence of the carboxylate ligand in **3**−**5** is also revealed in the Mo−N bond distances, which fall in the range 2.14−2.16 Å for the two formamidinate ligands *cis* to carboxylate, while the *trans* ligand has shorter bond lengths in the range 2.11−2.13 Å.

The bridged molecules **6**−**15** were readily prepared by the assembly of 2 equiv of $[Mo_2(DAniF)_3(MeCN)_2]^+$ with 1 equiv of the corresponding dicarboxylate, the product generally precipitating from MeCN in microcrystalline form in good yield. Compounds **6**, **8**, and **9** have been reported previously,[23] but pertinent data are presented here to facilitate discussion and comparison to other members of the family of bridged compounds with unsaturated linkers. All new compounds (**7**, **10**−**14**) were subject to structural characterization by X-ray crystallography (Table S3, Supporting Information).

In general, the structures can be described as having two chemically equivalent components, each having a quadruply bonded Mo_2 unit, linked by a dicarboxylate anion. Again the Mo−Mo distances are in a very narrow range and are approximately 2.09 Å. Generally, the Mo−N distances *trans* to the dicarboxylate anions are shorter than those for the corresponding *cis* ligands; however, the trend is not as marked as that found for **3**−**5**. All molecular pairs are diamagnetic, and

(44) Bera, J. K.; Fanwick, P. E.; Walton, R. A. *J. Chem. Soc., Dalton Trans.* **2001**, 109.

the two dimetal containing components are equivalent on the ^{1}H NMR time scale. For most compounds, the two methine signals for the *cis* and *trans* formamidinates are observable, but for those with the longest linkers, **13** and **14**, no such difference is noticeable.

Compounds **12**, **13**, and **14** all crystallize upon an inversion center in the space group $P\bar{1}$. Each successive addition of a −CH═CH− unit increases the separation between Mo_2 units by ∼2.2 Å to the maximum of 16.2 Å observed in **14**. Texate is the longest dicarboxylate linker thus far used in the assembly of M_2 units into larger arrays. The dicarboxylate linkers in **12**−**14** are comprised of alternating carbon−carbon double bonds and single bonds which do not differ in a statistically significant way[45] from values observed in the dimethyl esters (Table 3). This is consistent also with what has been observed in other systems in which transition metal ions are joined by polyolefinic bridging ligands of other types.[18d,46] Thermal ellipsoid plots of the core structures of molecules **12**−**14** are presented in Figure 3. It is noteworthy that the preparation of diffraction quality crystals for these compounds has required the use of a mixture of solvents from which the solvent molecule of optimal size and shape can be fit into the crystal interstices. The diffusion of a toluene/isooctane mixture into a 1,3-dichlorobenzene solution of **13**, for instance, succeeded in growing diffraction quality crystals, while the use of more common solvent combinations such as CH_2Cl_2/hexanes failed to produce material suitable for X-ray crystallography.

The maleate bridged molecule (**7**) shows rather significant distortion from planarity because of the steric crowding between *p*-anisyl groups of the formamidinate ligands on opposing Mo_2 units. The twist angle of 42.9° between the Mo_2 axes serves to alleviate some of the steric clash and undoubtedly is a feature that persists in solution. The *cis*,*cis*-muconate bridged molecule, **11**, is observed to have a relatively planar core geometry. It was found that solutions of **11** were susceptible to isomerization to the *trans*,*trans* isomer **12**, which was identified by crystallography. Successful crystallization of **11** required the use of concentrated solutions (to hasten crystal growth) that were maintained in the dark to avoid isomerization. Such rearrangement appears to be both a thermal and photoinduced process and is reminiscent of the *cis*−*trans* isomerization experienced by rhodopsin in the visual cycle.[47]

The allene-1,3-dicarboxylate bridged molecule, **10**, crystallizes as a racemic mixture in the orthorhombic space group *Fdd*2. The core structure of this molecule is depicted in Figure 4, the chiral configuration of the allene-1,3-dicarboxylate bridge being (*R*) and the twist angle between Mo_2 axes being 62.9°. The two halves of this molecule are related by a 2-fold axis passing through the central carbon atom of the allene unit, C(3). Molecule **10** appears to be the first transition metal compound in which allene-1,3-dicarboxylate binds transition metal ions through its carboxylate moieties, although other connectors such as allene and cumulene bridged polyphosphines have been used.[4a,48] The only existing examples of transition metal complexes containing the allene-1,3-dicarboxylate group are dinuclear rhenium,[49] manganese,[50] and ruthenium[51] carbonyl compounds in which allene-1,3-dicarboxylate dimethyl ester is observed in both μ-η^2-η^2 and μ-η^3-η^1 coordination modes involving the allenyl unit itself.

Table 4. Electrochemical Data[a] for Compounds **3**−**15**

cmpd	$E_{1/2}$ (+/0) (mV)	$E_{1/2}$ (2+/+) (mV)	$\Delta E_{1/2}$ (mV)	K_c[e]	ln K_c	d (Å)	1/*d*
3	351[b]						
4	217[b]						
5	225[b]						
6	294[b]	506[b]	212	3.8×10^3	8.3	6.953	0.144
7	209[c]	381[c]	172[d]	7.2×10^2	6.6	7.693	0.130
8	263[c]	408[c]	145[d]	2.0×10^2	5.3	9.194	0.109
9	325[c]	433[c]	150[d]	3.4×10^2	5.8	9.537	0.105
10	215[c]	345[c]	130[d]	1.6×10^2	5.1	9.395	0.106
11	293[c]	418[c]	125[d]	1.3×10^2	4.9	10.350	0.097
12	230[c]	335[c]	105[d]	60	4.1	11.575	0.086
13	194[c]	269[c]	75[d]	19	2.9	13.920	0.072
14	178[c]	243[c]	65[d]	13	2.5	16.156	0.062
15	225[c]	325[c]	100[d]	49	3.9	11.236	0.089

[a] These data were recorded on a CH Instruments model-CH1620A electrochemical analyzer in 0.1 M Bu_4NPF_6 solution (CH_2Cl_2) with Pt working and auxiliary electrodes and a Ag/AgCl reference electrode. The scan rate is 100 mV/s for CV and 2 mV/s for DPV. All the potential values are referenced to Ag/AgCl, and under the present experimental conditions, the $E_{1/2}(Fc^+/Fc)$ was consistently measured at 440 mV. [b] Obtained from CV. [c] These $E_{1/2}$ values were obtained from the relationship $E^1_{1/2} = E_c + (\Delta E_{1/2} + E_{pul})/2$ according to ref 7. $E^2_{1/2} = E^1_{1/2} + \Delta E_{1/2}$. E_c = the center potential of the DPV trace. $E_{pul} = 50$ mV. [d] Determined by the width-at-half-height method from the DPV traces according to Richardson and Taube, ref 7. Values are rounded to the nearest 5 mV. [e] K_c calculated from the formula $K_c = e^{\Delta E_{1/2}/25.69}$.

Electrochemistry and Electronic Communication. Electrochemical studies have shown that **3**−**15** can undergo one or two one-electron oxidations. The values of these oxidation potentials and other relevant data are presented in Table 4.

Each of the $Mo_2(DAniF)_3(O_2CR)$ complexes **3**−**5** displays a reversible one-electron oxidation at potentials (0.22−0.35 V) somewhat more oxidizing than that observed for the tetraformamidinate complex $Mo_2(DAniF)_4$ (0.15 V)[52] (Figure 5) and substantially less oxidizing than the potentials required to oxidize dimolybdenum tetracarboxylate complexes such as $Mo_2(2,4,6\text{-}Pr^i_3C_6H_2CO_2)_4$ (0.621 V).[53] These potentials correlate as expected with the basicity of the ligand set; that is, the more basic formamidinate ligand better supports the Mo_2^{5+} oxidation state and shifts the $Mo_2^{5+} \rightarrow Mo_2^{4+}$ potential to lower values as the number of formamidinate ligands increases. Within the set of complexes $Mo_2(DAniF)_3(O_2CR)$ (R = C≡CH, CH═CH_2) and $Mo_2(DAniF)_4$, the trend in $Mo_2^{5+} \rightarrow Mo_2^{4+}$ potentials (0.351 V, 0.217 V, 0.150 V) parallels the carboxylate and formamidinate ligand basicity (pK_a's of 1.89,[54] 4.25,[54] and 8.04,[55] respectively).

For the molecular pairs, there is a wider variation of the values of $E_{1/2}$, but it is significant that those with the longest unsaturated

(45) Taylor, J. R. *An Introduction to Error Analysis*; University Science Books: Sausalito, California, 1997.
(46) Gilbert, T. M.; Hadley, F. J.; Simmons, M. D.; Bauer, C. B.; Rogers, R. D. *J. Organomet. Chem.* **1996**, *510*, 83.
(47) Rando, R. R. *Chem. Rev.* **2001**, *101*, 1881.
(48) Hong, B. *Comments Inorg. Chem.* **1999**, *20*, 177.
(49) Adams, R. D.; Huang, M. *Organometallics* **1996**, *15*, 4437.
(50) Adams, R. D.; Huang, M. *Chem. Ber.* **1996**, *129*, 1447.
(51) Adams, R. D.; Huang, M.; Zhang, L. *J. Cluster Sci.* **1997**, *8*, 101.
(52) The $E_{1/2}$ of 0.150 V (Ag/AgCl) for the $Mo_2^{5+} \rightarrow Mo_2^{4+}$ process for $Mo_2(DAniF)_4$ obtained using our experimental conditions differs from a value previously published by another research group: Cf. Lin, C.; Protasiewicz, J. D.; Smith, E. T.; Ren, T. *Inorg. Chem.* **1996**, *35*, 6422. We will use our experimental number for reference.
(53) Cotton, F. A.; Daniels, L. M.; Hillard, E. A.; Murillo, C. A. *Inorg. Chem.* **2002**, *41*, 1639.
(54) Serjeant, E. P.; Dempsey, B. *Ionisation Constants of Organic Acids in Aqueous Solution*; Pergamon: Oxford, 1979.
(55) Oszczapowicz, J.; Orliński, R.; Hejchman, E. *Pol. J. Chem.* **1979**, *53*, 1259.

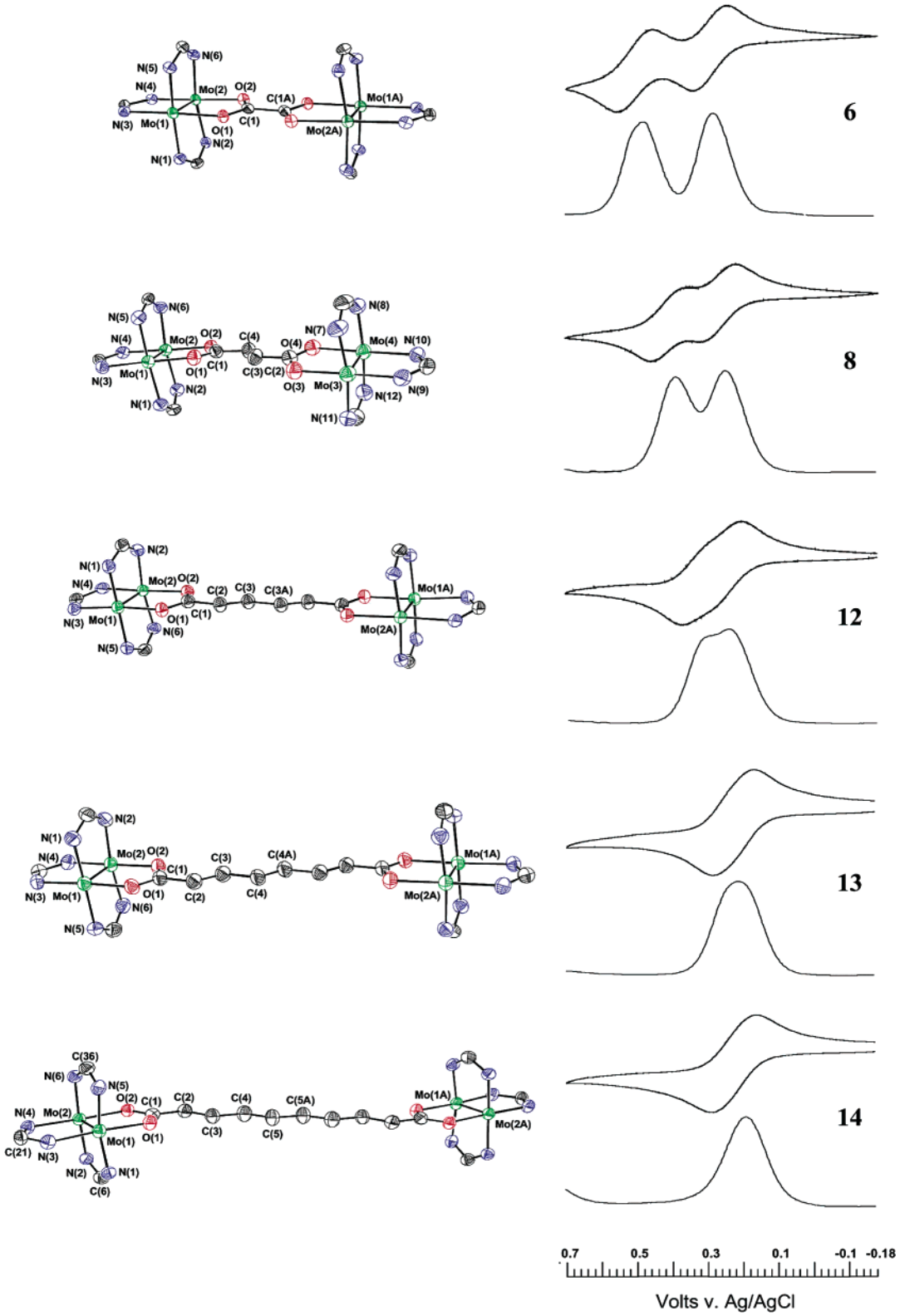

Figure 3. Core structures and electrochemistry results for molecules **6**, **8**, **12**, **13**, and **14**. Molecules **6** and **8** were previously reported[23] and are included here for comparison. Ellipsoids are shown at the 50% probability level, and all *p*-anisyl groups and hydrogen atoms are omitted for clarity.

linkers, **13** and **14**, possess first oxidation potentials of less than 200 mV, making them the most easily oxidized dimolybdenum pairs having a mix of formamidinate and carboxylate ligands. Using differential pulse voltammetry, DPV, the two processes are clearly distinguishable in those compounds with shorter linkers, for example, for **6** and **8** (Figure 3). However, as the linkers become longer, the two peaks begin to merge and finally they appear as one. Nevertheless, values for $\Delta E_{1/2}$, the separation between successive one-electron oxidations, can be determined using standard techniques such as the width-at-half-height method of Richardson and Taube.[7] These values are presented Table 4.

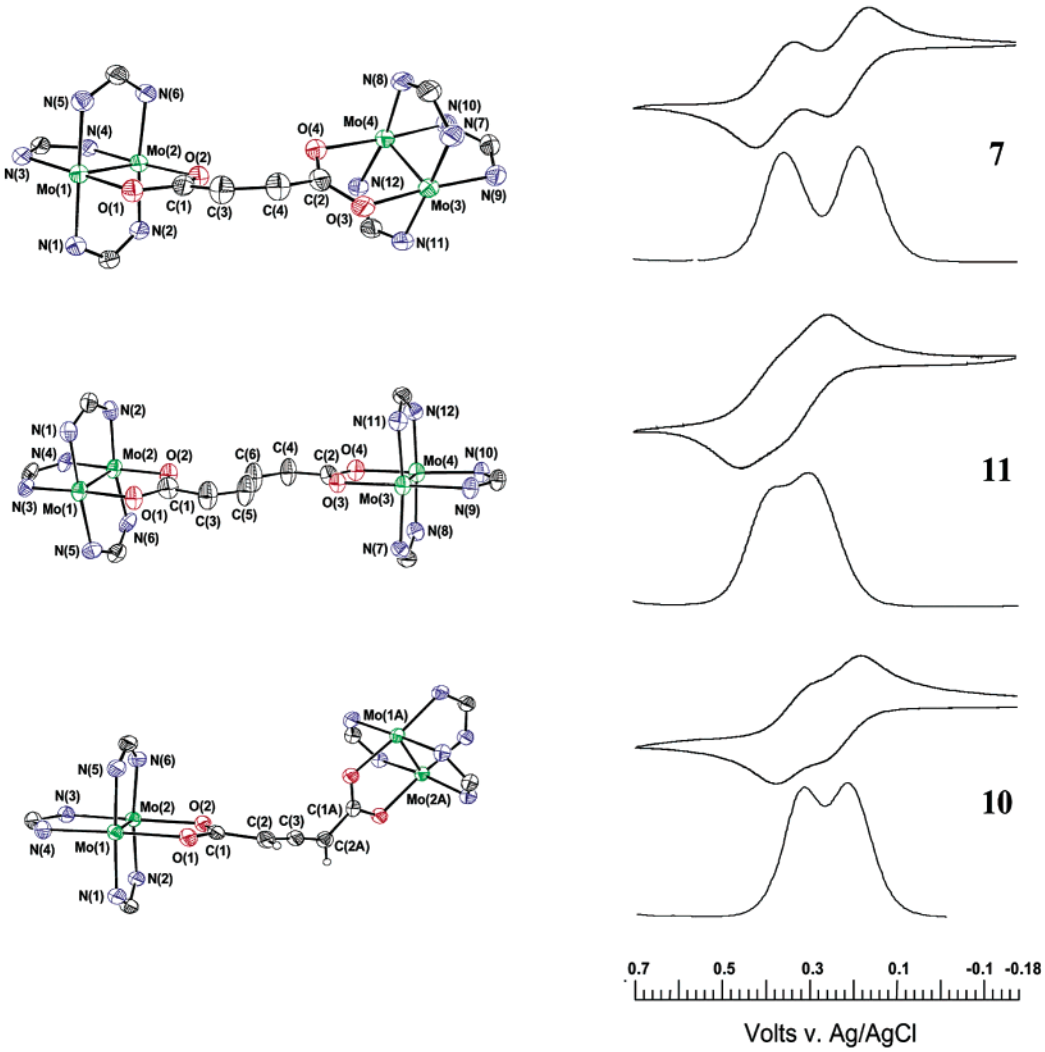

Figure 4. Core structures and electrochemistry results for molecules **7**, **11**, and **10**. Ellipsoids are shown at the 50% probability level, and all *p*-anisyl groups and hydrogen atoms are omitted for clarity.

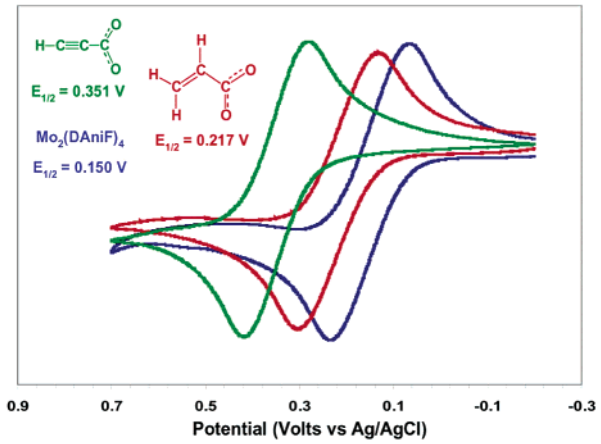

Figure 5. Overlay cyclic voltammograms for the molecules $Mo_2(DaniF)_4$, **3**, and **4**, illustrating the dependence of the Mo_2^{5+}/Mo_2^{4+} redox couple upon the basicity of the ligand set.

$\Delta E_{1/2}$ in systems with two redox centers depends inversely upon the distance, a relationship which derives from electric potential energy expressed in terms of the distance between two point charges. Figure 6 is a plot of $\Delta E_{1/2}$ versus *d*, where *d* is the distance between the centers of the Mo_2 units, as determined crystallographically, for the compounds we have previously reported[23] as well as for those in the present work.[56] These dicarboxylate linked molecules are identified numerically according to the system shown in Chart 1, where only the linker is illustrated. The section outlined in blue circumscribes those molecules with linkers which are chemically saturated or otherwise not expected to be effective transmitters of the effect of oxidation of one Mo_2 unit upon the other. Transmission of the effect of oxidation of one Mo_2 unit upon the other is essentially a through-space, electrostatic phenomenon. Deviations from linearity may be attributed at least in part to plausible differences in *d* between the crystalline state and solution. A molecule with a flexible linker such as $-CH_2CH_2-$ might have a value of *d* effectively longer in solution than that observed in the crystal structure. Interestingly, the allene-1,3-dicarboxylate bridged molecule, **10**, is included in this set of compounds having poor communication through the linker. This is likely due to the discontinuity imposed on its π system by the orthogonal set of MOs. This result is entirely consistent with the observation of Hong et al. that found no communication between an Os and a Ru unit linked by 1,1′,3,3′-tetrakis-(diphenylphosphino)allene.[4a]

(56) In ref 23, a plot of $\Delta E_{1/2}$ versus d^2 was used instead. However, the general appearance of the plot of $\Delta E_{1/2}$ versus *d* is similar to that of the published figure. More importantly, the discussion presented in ref 23 is not affected.

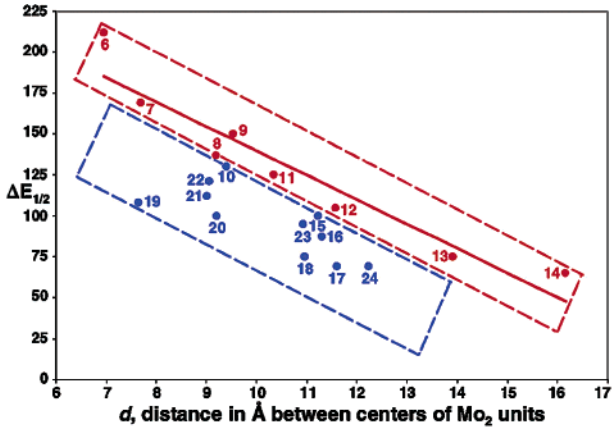

Figure 6. Plot of $\Delta E_{1/2}$ vs d for the compounds $[Mo_2(DAniF)_3]_2(\mu\text{-}O_2CXCO_2)$, where d is the distance in Å between the centers of the Mo_2 units. The series in blue is the set of compounds whose dicarboxylate linkers are not good communicators of the effect of one oxidation upon the other Mo_2 unit. The series in red is the set of compounds with unsaturated, conjugated linkers. A best fit line for the series in red is shown, with a correlation coefficient of 0.91. $\Delta E_{1/2}$ values are obtained from the differential pulse voltammograms by the width-at-half-height method of Richardson and Taube.[7]

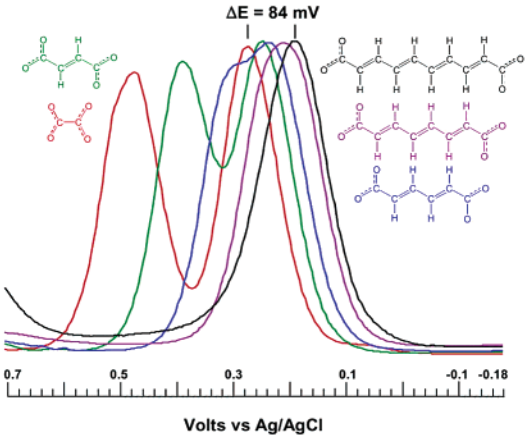

Figure 7. Overlay differential pulse voltammograms for the series $Mo_2(DAniF)_3(\mu\text{-}O_2C(CH{=}CH)_nCO_2)$, where $n = 0-4$, showing the increasing ease of oxidation with increasing length of the dicarboxylate linker.

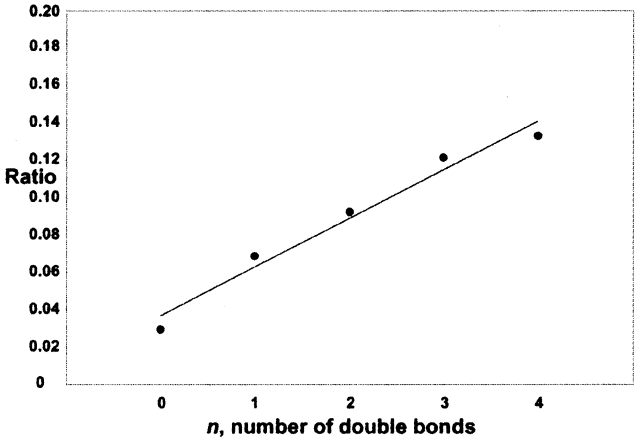

Figure 8. Plot of the ratio of the contribution made to the composition of the highest occupied molecular orbital by the atoms of the bridging dicarboxylate over the contribution made by the remaining atoms of the molecule as a function of n in the series $[Mo_2(DAniF)_3]_2(\mu\text{-}O_2C(CH{=}CH)_n\text{-}CO_2)$, where $n = 0-4$.

The area bounded in red encompasses those molecules with unsaturated, conjugated linkers. That this region lies well above the one in blue strongly suggests that factors other than mere electrostatics are at work here. Undoubtedly, an important contributor is the presence of the conjugated π system, which provides a relatively soft set of polarizable bonds through which the increase in the positive charge upon oxidation may be felt by one Mo_2 unit from the other, therefore giving rise to a considerable increase in internuclear communication between the Mo_2 units. It is also true (vide infra) that the atomic orbitals of these linkers contribute to the molecular orbitals from which electrons are removed. Included for the points in red is also a best fit line, for which the correlation coefficient is 0.91.

The electrochemical behavior of the series of compounds **6**, **8**, **12**, **13**, and **14**, in which the two Mo_2 units are linked by an unsaturated, conjugated dicarboxylate according to the formula $[Mo_2(DAniF)_3](O_2C(CH{=}CH)_nCO_2)[Mo_2(DAniF)_3]$ ($n = 0-4$), reveals the effect of increasing the length of the conjugated π system. An overlay of the DPV traces of these five compounds is shown in Figure 7. The most obvious observation is the merging of the separate one-electron waves into a single wave in which the resolution has disappeared. A second, more subtle feature is the small shift toward milder oxidizing potentials for the first observed oxidation. Oxidation of the texate linked molecule ($n = 4$) occurs more easily by 84 mV compared to the first oxidation of the oxalate linked molecule, and the first oxidations of the remaining molecules are more or less evenly spaced between these two. This result is consistent with the general observation that the separations between energy levels continually diminish in conjugated π systems of increasing length. It has been noted, for instance, that conjugated polyolefins terminated by *tert*-butyl substituents[57] or by ylidene-1,3-dithiole-4,5-dicarbonitrile groups,[58] as well as conjugated *o*-phenylene vinylene oligomers,[59] are increasingly easier *both* to oxidize *and* to reduce as the length of the system is increased. Voltammetric studies upon carotenoids also reveal an increasing ease of oxidation as the polyolefinic chain is lengthened in addition to a progressively smaller separation between the first oxidation and a second one.[60]

As discussed in more detail in the following paper,[24] DFT calculations have been employed to determine the electronic structure of the compounds reported here. An examination of the character of the highest occupied molecular orbital in the series $[Mo_2(DAniF)_3](O_2C(CH{=}CH)_nCO_2)[Mo_2(DAniF)_3]$ ($n = 0-4$) reveals that the contribution of the bridging dicarboxylate to the composition of this MO increases steadily with n. When this contribution by the dicarboxylate ligand atomic orbitals to the makeup of the HOMO is expressed as a ratio to the contribution made by the remaining atoms in the molecule and then plotted against the increase in n (Figure 8), an approximately linear relationship emerges. The relative involvement of these bridging dicarboxylate ligands in the HOMO

(57) Kiehl, A.; Eberhardt, A.; Adam, M.; Enkelmann, V.; Müllen, K. *Angew. Chem., Int. Ed. Engl.* **1992**, *31*, 1588.
(58) Märkl, G.; Pöll, A.; Aschenbrenner, N. G.; Schmaus, C.; Troll, T.; Kreitmeier, P.; Nöth, H.; Schmidt, M. *Helv. Chim. Acta* **1996**, *79*, 1497.
(59) Gebhardt, V.; Bacher, A.; Thelakkat, M.; Stalmach, U.; Meier, H.; Schmidt, H.-W.; Haarer, D. *Adv. Mater.* **1999**, *11*, 119.
(60) Deng, Y.; Gao, G.; He, Z.; Kispert, L. D. *J. Phys. Chem. B* **2000**, *104*, 5651.

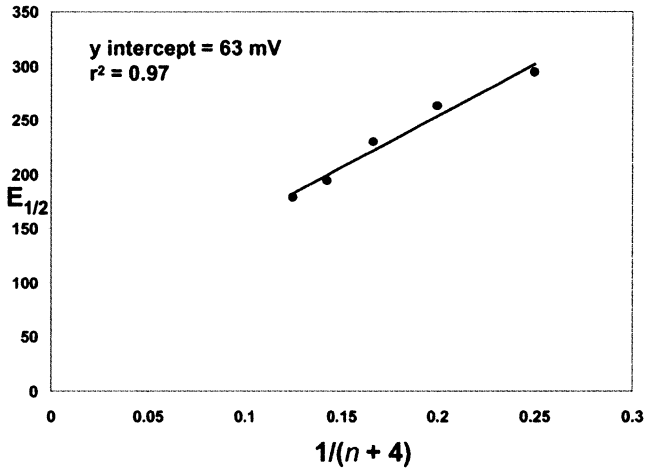

Figure 9. Plot of the first oxidation potential $E_{1/2}$ for the series $[Mo_2(DAniF)_3]_2(\mu\text{-}O_2C(CH{=}CH)_nCO_2)[Mo_2(DAniF)_3]$ ($n = 0-4$) vs $1/(n + 4)$. Each Mo_2^{4+} unit and carboxylate group is counted as an additional part of the conjugated system.

grows more than 3-fold as n varies from 0 to 4, which appears consistent with the trend toward milder oxidizing potentials seen in Figure 7.

For soluble oligomers containing conjugated systems, an important trend has been observed in relation to the chain length. In such compounds, the redox potentials converge toward a limiting potential which is characteristic of the conjugated polymer, and plots of $E_{1/2}$ versus the inverse of the chain length ($1/n$) always show a linear dependence. Here, n is the number of conjugated bonds. The limit $1/n = 0$ provides an estimate of the first redox potential of a hypothetical polymer consisting of an infinitely long chain in a solution (E_∞).[61] If we treat **6**, **8**, **12**, **13**, and **14** as the first members of a chain of conjugated multiple bonds, we find that for the first oxidation process a plot of E versus $1/n$, where n is number of double bonds in the dicarboxylate, is not linear. Neither is a similar plot that includes the number of carboxylate groups. However, a linear relationship is apparent when the multiple bonds from the Mo_2 units are added to the number of bonds from the chain and the number of carboxylate groups, which suggests that there exists a very significant modulation of the linkers by the multiply bonded Mo_2 units (Figure 9). From the y-intercept, it can be estimated that the $E_{1/2}$ for the first oxidation of the corresponding molecular pair having an infinitely long linker will be ~63 mV.

Comproportionation Constants. A fundamental parameter in systems in which two separate but otherwise identical redox centers exist in the same molecule is the comproportionation constant K_c, defined as the equilibrium constant for the reaction $[M^n{-}M^n] + [M^{(n+1)}{-}M^{(n+1)}] \leftrightarrows 2[M^n{-}M^{(n+1)}]$.[8a,62] Thus, K_c is a measure of the degree to which a mixed valent species $[M^n{-}M^{(n+1)}]$, which may, of course, be localized as written or be delocalized, is favored relative to the unoxidized and doubly oxidized species. K_c assumes the statistical value of 4 when the two redox sites are completely independent and noninteracting and goes to much higher values as electrostatic interaction or charge delocalization increases. It may be determined by different methods. For example, if the mixed valent species $[M^n{-}M^{(n+1)}]$ has an intervalence absorption band that is not overlapped by absorption bands belonging to the other species, then a spectrophotometric titration and analysis of the apparent extinction coefficients as a function of oxidizing or reducing equivalents permits one to measure a value for K_c.[63] A less obvious but often more convenient alternative is the measurement of K_c electrochemically. K_c depends on $\Delta E_{1/2}$, the difference between the first and second ionization potentials, according to the relationship $K_c = e^{\Delta E_{1/2}/25.69}$ (298 K, $\Delta E_{1/2}$ in mV),[7,8a] which leads to a limiting value of 36 mV for $\Delta E_{1/2}$ when $K_c = 4$. Thus, even two well separated and noninteracting redox centers will have a nonzero $\Delta E_{1/2}$, but $\Delta E_{1/2}$ will increase rapidly with increasing interaction.

The calculated values of K_c, shown in Table 4, clearly indicate that, for the conjugated linkers, the electronic communication between Mo_2 units is significantly higher through the shorter linkers, for example, oxalate in **6**, than through the longer linkers, for example, tamuate in **14**.

Isomerization of $[Mo_2(DAniF)_3](\mu\text{-}cis,cis\text{-}O_2C(CH{=}CH)_2CO_2)[Mo_2(DAniF)_3]$. The photoinduced *cis*-to-*trans* rearrangement of conjugated polyolefins is an isomerization reaction of physiological significance, for example, in the isomerization of polyunsaturated fatty acids. Also, by such a process, rhodopsin undergoes a *cis*−*trans* conversion, which is a key element in the visual transduction pathway.[47] Such photoisomerizations of polyolefins are a general phenomenon, and in the particular case of *cis*,*cis*-muconic acid, its photosensitivity was noted many years ago.[64] Our finding that the *cis*,*cis*-muconate linked compound, **11**, was susceptible to isomerization to the *trans*,*trans*-muconate linked molecule, **12**, led us to undertake a qualitative comparison between the rates of isomerization of **11** and dimethyl *cis*,*cis*-muconate to ascertain what effect coordination to the Mo_2^{4+} units had upon the process.

Samples of both compounds were prepared in NMR tubes and dissolved in CD_2Cl_2 and irradiated at each of two different wavelengths. At 254 nm over a period of 48 h, **11** underwent negligible isomerization to **12**, as determined by ^1H NMR, although a small amount of decomposition was visible. Under the same conditions, pure dimethyl *cis*,*cis*-muconate was found to have converted to a mixture with the *trans*,*trans* isomer, the two isomers existing in a 3:2 ratio (*cis*,*cis*:*trans*,*trans*). A minor amount of another species was observed, possibly the *cis*,*trans*-isomer of dimethyl muconate, although that assignment was not confirmed by independent preparation of an authentic sample. During the same period, irradiation at 365 nm produced a 1:2.4 mixture of **11**:**12** with some degradation to unidentified species, while the dimethyl ester of *cis*,*cis*-muconate was found in a 1:3 ratio with the *trans*,*trans* isomer. At both wavelengths examined, **11** underwent a slower isomerization than did dimethyl *cis*,*cis*-muconate, but this difference was more pronounced at the shorter wavelength.

Conclusions and Summary

The present work has extended the set of dicarboxylate linked molecules of the type $[Mo_2(DAniF)_3](O_2CXCO_2)[Mo_2(DAniF)_3]$ to include new members with highly unsaturated linkers. Among these are the molecules $[Mo_2(DAniF)_3](O_2C(CH{=}CH)_nCO_2)$-

(61) Heinze, J.; Tschuncky, P. In *Electronic Materials: The Oligomer Approach*; Müllen, K.; Wegner, G., Eds.; Wiley-VCH: New York, 1998; Chapter 9.
(62) Kaim, W.; Klein, A.; Glöckle, M. *Acc. Chem. Res.* **2000**, *33*, 755.
(63) Demadis, K. D.; Hartshorn, C. M.; Meyer, T. J. *Chem. Rev.* **2001**, *101*, 2655.
(64) (a) Elvidge, J. A.; Linstead, R. P.; Sims, P.; Orkin, B. A. *J. Chem. Soc.* **1950**, 2235. (b) Elvidge, J. A.; Linstead, R. P.; Sims, P. *J. Chem. Soc.* **1953**, 1793.

$[Mo_2(DAniF)_3]$ ($n = 2-4$), which, with the oxalate and fumarate linked molecules prepared earlier, comprise a homologous series ($n = 0-4$) in which the effect of increasing n upon physical properties can be examined. Another variation we have studied is that between the pairs of geometrical isomers **7**/**8** and **11**/**12**. For comparison, we have also prepared the unbridged compounds $Mo_2(DAniF)_3(O_2CCH{=}CH_2)$ and $Mo_2(DAniF)_3((E)\text{-}O_2CCH{=}CH{-}CH{=}CH_2)$. All new dimolybdenum compounds have been structurally characterized by X-ray crystallography, as have the dimethyl esters of many of the organic dicarboxylates.

The molecules $[Mo_2(DAniF)_3](O_2CXCO_2)[Mo_2(DAniF)_3]$ have been examined by cyclic and differential pulse voltammetry. The upshot of this study is that the compounds in which the dicarboxylate linker is an *unsaturated, conjugated bridge* constitute a set in which electrochemical communication from one Mo_2 unit to the other is stronger and more persistent over distance than is accounted for by a purely electrostatic interaction. This electrochemical communication is quantified by measuring $\Delta E_{1/2}$ values, the separation between successive one-electron oxidations of the separate Mo_2 units. In the series $[Mo_2(DAniF)_3](O_2C(CH{=}CH)_nCO_2)[Mo_2(DAniF)_3]$ ($n = 0-4$), the first oxidation potential shifts progressively (albeit slightly) to less positive values, an effect that is attributed to an increasing contribution by the polyolefinic α,ω-dicarboxylate to the molecular orbital undergoing oxidation. For the same set of five molecules, a plot of the first oxidation potential, $E_{1/2}$, versus $1/(n + 4)$, where the two carboxylate groups and the two Mo_2 units are included with n as parts of the conjugated system, produces a linear relationship from which an estimate of $E_{1/2}$ as n becomes very large may be obtained.

One of the stimuli for the present work was the observation of the similarity between simple polyolefinic α,ω-dicarboxylic acids and certain carotenoids, a topic that will be dealt with in more detail in the following paper.[24] We have thus investigated the efficacy of electrochemical and spectroscopic communication mediated by a dicarboxylic polyolefinic connector with the hope that some of our results may bear some relevance to biological systems. Our perspective part of the time has rested in deepening our understanding of how the properties of and communication between Mo_2 units is determined by the length and degree of unsaturation of the linker, but we may also invert our viewpoint and inquire how the polyolefinic dicarboxylate is perturbed by coordination to the Mo_2 unit. We have seen, for instance, that while $[Mo_2(DAniF)_3](\mu\text{-}cis,cis\text{-}O_2C(CH{=}CH)_2CO_2)[Mo_2(DAniF)_3]$ undergoes a photoinduced isomerization to the *trans,trans* isomer, that rearrangement is slowed relative to the dimethyl ester of the same dicarboxylic acid. This effect may be due to a shift in UV absorption maxima for $[Mo_2(DAniF)_3](cis,cis\text{-}O_2C(CH{=}CH)_2CO_2)[Mo_2(DAniF)_3]$ compared to dimethyl *cis,cis*-muconate, which suggests that polyolefinic systems might be photostabilized or tuned in optical sensitivity by coordination to an appropriate transition metal ion.

Interest has been growing in polyene systems, including those which incorporate transition metals, as components for light harvesting devices[65] and materials with enhanced nonlinear optical properties.[18d,46] In view of this increasing activity, it is rather surprising that no use appears to have been made of the polyolefinic α,ω-dicarboxylic acids $HO_2(CH{=}CH)_nCO_2H$ where $n \geq 3$. Considering that carboxylates are ubiquitous ligands in transition metal chemistry, we imagine other applications for these particular diacids, such as their incorporation into other types of supramolecular assemblies or their use as modifiers of the electrooptical properties of a transition metal ion. Among several current avenues of research in this laboratory is the use of these polyolefinic α,ω-dicarboxylic acids in the preparation of the molecular squares $[Mo_2(DAniF)_2]_4(\mu\text{-}O_2C(CH{=}CH)_nCO_2)_4$ ($n = 2-4$). Such squares will likely have interesting electrochemical behavior and electronic spectra.

Acknowledgment. We thank the National Science Foundation and the Welch Foundation for funding the research reported here. J.P.D. acknowledges the support of an NIH postdoctoral fellowship. We thank Dr. Kim Dunbar for access to the Shimadzu UV-1601PC spectrophotometer with which the absorption spectra were taken. The contribution of Lisa M. Pérez in performing and interpreting the DFT calculations, which permitted an assessment of the bridging dicarboxylate contribution to the electrochemical oxidations, is gratefully acknowledged. We also thank Dr. Marcos Shulte and Ms. Anya Dilley for translations of several preparations and procedures from the German literature.

Supporting Information Available: Accessible to those interested are thermal ellipsoid drawings at the 50% probability levels with complete atomic labeling in PDF in addition to X-ray crystallographic data in CIF format. Tables summarizing the unit cell parameters and refinement statistics for all the crystal structures presented herein, as well as a table with selected bond distances and angles for the organic molecules that were structurally characterized, are also available. This material is available free of charge via the Internet at http://pubs.acs.org.

JA029101I

(65) (a) Gust, D.; Moore, T. A.; Moore, A. L.; Barrett, D.; Harding, L. O.; Makings, L. R.; Liddell, P. A.; De Schryver, F. C.; Van der Auweraer, M.; Bensasson, R. V.; Rougée, M. *J. Am. Chem. Soc.* **1988**, *110*, 321. (b) Gust, D.; Moore, T. A.; Moore, A. L.; Lee, S.-J.; Bittersmann, E.; Luttrull, D. K.; Rehms, A. A.; DeGraziano, J. M.; Ma, X. C.; Gao, F.; Belford, R. E.; Trier, T. T. *Science* **1990**, *248*, 199. (c) Hung, S.-C.; Macpherson, A. N.; Lin, S.; Liddell, P. A.; Seely, G. R.; Moore, A. L.; Moore, T. A.; Gust, D. *J. Am. Chem. Soc.* **1995**, *117*, 1657. (d) Liddell, P. A.; Kuciauskas, D.; Sumida, J. P.; Nash, B.; Nguyen, D.; Moore, A. L.; Moore, T. A.; Gust, D. *J. Am. Chem. Soc.* **1997**, *119*, 1400.